

# Robust Blockwise Random Pivoting: Fast and Accurate Adaptive Interpolative Decomposition

Yijun Dong\*      Chao Chen<sup>†</sup>      Per-Gunnar Martinsson<sup>‡</sup>  
Katherine Pearce<sup>§</sup>

## Abstract

The interpolative decomposition (ID) aims to construct a low-rank approximation formed by a basis consisting of row/column skeletons in the original matrix and a corresponding interpolation matrix. This work explores fast and accurate ID algorithms from five essential perspectives for empirical performance: (a) skeleton complexity that measures the minimum possible ID rank for a given low-rank approximation error, (b) asymptotic complexity in FLOPs, (c) parallelizability of the computational bottleneck as matrix-matrix multiplications, (d) error-revealing property that enables automatic rank detection for given error tolerances without prior knowledge of target ranks, (e) ID-revealing property that ensures efficient construction of the optimal interpolation matrix after selecting the skeletons. While a broad spectrum of algorithms have been developed to optimize parts of the aforementioned perspectives, practical ID algorithms proficient in all perspectives remain absent. To fill in the gap, we introduce *robust blockwise random pivoting (RBRP)* that is parallelizable, error-revealing, and exact-ID-revealing, with comparable skeleton and asymptotic complexities to the best existing ID algorithms in practice. Through extensive numerical experiments on various synthetic and natural datasets, we empirically demonstrate the appealing performance of RBRP from the five perspectives above, as well as the robustness of RBRP to adversarial inputs.

## 1 Introduction

Interpolative decomposition (ID) is a special type of low-rank approximation where the basis of the row/column space consists of the rows/columns in the original matrix. This allows ID to capture the essential structures and relationships within the data. ID has found applications in various fields, including numerical analysis, data compression, and machine learning, where preserving the integrity of the original data is of paramount importance.

---

\*Courant Institute, New York University (yd1319@nyu.edu).

<sup>†</sup>Department of Mathematics, North Carolina State University (cchen49@ncsu.edu).

<sup>‡</sup>Department of Mathematics & Oden Institute, University of Texas at Austin (pgm@oden.utexas.edu).

<sup>§</sup>Oden Institute, University of Texas at Austin (katherine.pearce@austin.utexas.edu).

Given a data matrix  $\mathbf{X} = [\mathbf{x}_1, \dots, \mathbf{x}_n]^T \in \mathbb{R}^{n \times d}$  consisting of  $n$  data points  $\{\mathbf{x}_i \in \mathbb{R}^d\}_{i \in [n]}$ , along with a constant  $\epsilon > 0$  and a target rank  $r \in \mathbb{N}$ , we aim to construct a  $(r, \epsilon)$ -ID of  $\mathbf{X}$ :

$$\underset{n \times d}{\mathbf{X}} \approx \underset{n \times k}{\mathbf{W}} \underset{k \times d}{\mathbf{X}_S} \quad \text{s.t.} \quad \|\mathbf{X} - \mathbf{W}\mathbf{X}_S\|_F^2 \leq (1 + \epsilon) \|\mathbf{X} - \mathbf{X}_{\langle r \rangle}\|_F^2 \quad (1)$$

where (i)  $k$  is the (unknown) target rank; (ii)  $\mathbf{X}_{\langle r \rangle}$  is the optimal rank- $r$  approximation of  $\mathbf{X}$  (given by the singular value decomposition (SVD)); (iii)  $S = \{s_1, \dots, s_k\} \subset [n]$  are the skeleton indices corresponding to the *row skeleton* submatrix  $\mathbf{X}_S = [\mathbf{x}_{s_1}, \dots, \mathbf{x}_{s_k}]^T \in \mathbb{R}^{k \times d}$ ; and (iv)  $\mathbf{W} \in \mathbb{R}^{n \times k}$  is an *interpolation matrix* with (nearly) optimal error  $\|\mathbf{X} - \mathbf{W}\mathbf{X}_S\|_F^2$  for the given  $\mathbf{X}_S$ . The construction of an ID can be divided into two stages:

- (i) selecting a skeleton subset  $S \subset [n]$  that achieves a small *skeletonization error*

$$\mathcal{E}_{\mathbf{X}}(S) \triangleq \left\| \mathbf{X} - \mathbf{X}\mathbf{X}_S^\dagger \mathbf{X}_S \right\|_F^2 = \min_{\mathbf{W} \in \mathbb{R}^{n \times |S|}} \|\mathbf{X} - \mathbf{W}\mathbf{X}_S\|_F^2; \quad (2)$$

- (ii) given  $S$ , computing an interpolation matrix  $\mathbf{W} \in \mathbb{R}^{n \times |S|}$  efficiently<sup>1</sup> that (approximately) minimizes the *interpolation error*:  $\mathcal{E}_{\mathbf{X}}(\mathbf{W} | S) \triangleq \|\mathbf{X} - \mathbf{W}\mathbf{X}_S\|_F^2$ .

In this work, we explore fast and accurate ID algorithms from both the skeleton subset and the interpolation matrix perspectives, starting by posing the main question:

*How to construct a  $(r, \epsilon)$ -ID efficiently with as few skeletons  $S$  as possible, without prior knowledge of the target rank  $k$ ?*

## 1.1 What are Fast and Accurate ID Algorithms?

To formalize the concept of “fast and accurate” ID algorithms, we dissect the above main question into the following properties, together providing systematic performance measurements for ID algorithms from both the efficiency and accuracy perspectives.

- (a) **Skeleton complexity** measures the minimum number of skeletons (*i.e.*, the minimum possible rank of ID) that an algorithm must select before  $\mathcal{E}_{\mathbf{X}}(S) \leq (1 + \epsilon) \|\mathbf{X} - \mathbf{X}_{\langle r \rangle}\|_F^2$  (*i.e.*, where there exists a  $(r, \epsilon)$ -ID associated with  $S$ ).
- (b) **Asymptotic complexity** measures the number of floating point operations (FLOPs) in the skeleton selection process of the algorithm asymptotically.
- (c) **Parallelizability** (in the context of this work) refers to the implementation advantage that the dominant cost for skeleton selection in the algorithm appears as matrix-matrix, instead of matrix-vector, multiplications with  $\mathbf{X}$ . Thanks to the widely available high-performance implementation (*e.g.*, Level 3 BLAS [19]), matrix-matrix multiplications are much faster than matrix-vector multiplications in practice under the same asymptotic complexity.

---

<sup>1</sup>It is worth clarifying that although Equation (2) directly provides  $\mathbf{W} = \mathbf{X}\mathbf{X}_S^\dagger$  as the minimizer of  $\min_{\mathbf{W}} \mathcal{E}_{\mathbf{X}}(\mathbf{W} | S) = \mathcal{E}_{\mathbf{X}}(S)$ , the explicit computation of  $\mathbf{X}\mathbf{X}_S^\dagger$  takes  $O(ndk + dk^2 + nk^2)$  time (*e.g.*, via Equation (9)), where the dominant cost  $O(ndk)$  is undesired. Therefore, whenever available, information from the skeleton selection process is usually leveraged to evaluate/approximate  $\mathbf{W}$  efficiently in  $o(ndk)$  time (as elaborated in Section 5), which may lead to the gap  $\mathcal{E}_{\mathbf{X}}(\mathbf{W} | S) - \mathcal{E}_{\mathbf{X}}(S) > 0$ .

- (d) **Error-revealing property** refers to the ability of an algorithm to evaluate the skeletonization error efficiently on the fly so that the target rank  $k$  does not need to be given a priori.

**Definition 1.1** (Error-revealing). *An ID algorithm is error-revealing if after selecting a skeleton subset  $S$ , it can evaluate  $\mathcal{E}_{\mathbf{X}}(S)$  efficiently with at most  $O(n)$  operations.*

That is, given any relative error tolerance  $\tau \in (0, 1)$ , an error-revealing ID algorithm can determine an appropriate rank  $k$  with negligible additional cost (*i.e.*, no more than  $O(nk)$ ) while selecting a skeleton subset  $S$  ( $|S| = k$ ) such that  $\mathcal{E}_{\mathbf{X}}(S) \leq \tau \|\mathbf{X}\|_F^2$ . For the sake of analysis, we define a useful constant concerning  $\mathbf{X}$  throughout the paper:

$$\eta_r \triangleq \|\mathbf{X} - \mathbf{X}_{\langle r \rangle}\|_F^2 / \|\mathbf{X}\|_F^2, \quad (3)$$

which quantifies the relative tail weight of  $\mathbf{X}$  with respect to the rank  $r$  and represents the relative optimal rank- $r$  approximation error of  $\mathbf{X}$ . Notice that when  $\tau < (1 + \epsilon)\eta_r$ , the algorithm outputs an  $(r, \epsilon)$ -ID.

- (e) **ID-revealing property** characterizes whether the skeleton selection stage of an ID algorithm generates sufficient information for efficient interpolation matrix construction.

**Definition 1.2** (Exact/inexact/non-ID-revealing). *We call a skeleton selection algorithm exact-ID-revealing if it contains sufficient information in addition to  $S$  such that the optimal interpolation matrix  $\mathbf{W} = \mathbf{X}\mathbf{X}_S^\dagger$  can be evaluated exactly and efficiently in  $O(nk^2)$  time. Otherwise, if a suboptimal interpolation matrix  $\mathbf{W} \approx \mathbf{X}\mathbf{X}_S^\dagger$  can be constructed in  $O(nk^2)$  time, we say that the skeleton selection algorithm is inexact-ID-revealing. If neither  $\mathbf{X}\mathbf{X}_S^\dagger$  nor its approximations can be constructed in  $O(nk^2)$  time, the skeleton selection algorithm is non-ID-revealing.*

## 1.2 How to Combine Adaptiveness and Randomness for ID?

Adaptiveness and randomness are two critical algorithmic properties that can be leveraged to characterize a skeleton selection algorithm. On one hand, with adaptiveness, the skeleton selection in each step is aware of the selected skeletons from the previous steps so that redundant skeleton selection can be better avoided. On the other hand, randomness diversifies the skeleton selection, thereby improving the robustness of algorithms to scarce adversarial inputs and providing strong statistical guarantees for skeleton complexities.

To ground the notions of adaptiveness and randomness, we synopsise some representative existing skeleton selection algorithms below, as well as in Table 1, with a focus on the aforementioned properties for performance measurement.

- (a) **Greedy pivoting** is a classical strategy in numerical linear algebra that involves *only adaptiveness*. As an example of greedy pivoting, column-pivoted QR (CPQR) [18, Section 5.4.2] picks the point in the residual with the maximum norm in each step and adaptively updates the residual via projection onto the orthogonal complement of the skeletons. Despite the error-revealing and exact-ID-revealing abilities, along with the remarkable empirical success, of CPQR, deterministic greedy pivoting algorithms like CPQR are inherently sequential and vulnerable to adversarial inputs where the skeleton complexity approaches the problem size  $n$  [5, 25].

- (b) **Sampling** is a widely studied set of skeleton selection methods that involve *only randomness*. Some common examples related to ID include squared-norm sampling [13], leverage score sampling [29], and DPP sampling [2, 10, 27]. As a trade-off between the skeleton complexity and efficiency, the fast ( $O(nd)$ -time) sampling methods like squared-norm sampling tend to suffer from high skeleton complexities that depend heavily on the matrix [5, 13]; whereas constructions of the more sophisticated distributions like leverage score and DPP are usually expensive [9, 16, 23]. Moreover, for ID, sampling methods generally fail to be error-revealing or ID-revealing.
- (c) **Random pivoting** combines adaptiveness and randomness by replacing the greedy selection of maximum norm in CPQR with random sampling according to the squared-norm distribution associated with the residual [5, 12, 13]. Closely related to the ID problem considered in this work, the idea of random pivoting is revitalized by the inspiring recent work [5] in the context of column Nyström approximation with a nearly optimal skeleton complexity guarantee [5, Theorem 3.1]. However, analogous to CPQR, although random pivoting enjoys the desired error-revealing and exact-ID-revealing properties, the sequential nature of random pivoting compromises its efficiency in practice.
- (d) **Sketchy pivoting** is an alternative combination of adaptiveness and randomness that randomly embeds the row space of  $\mathbf{X}$  via sketching [22, 46], on the top of which skeletons are selected via greedy pivoting [15, 45]. In contrast to random pivoting, the cost of sketchy pivoting is dominated by the embarrassingly parallelizable sketching process. As a trade-off for the superior empirical efficiency, sketchy pivoting sacrifices the error-revealing property since sketching requires prior knowledge of the target  $k$  (or its overestimation)<sup>2</sup>. Furthermore, sketchy pivoting is inexact-ID-revealing due to the loss of information during sketching. As a simple effective remedy for the loss of accuracy, we observe that multiplicative oversampling can remarkably improve the gap between the interpolation and skeletonization error  $\mathcal{E}_{\mathbf{X}}(\mathbf{W} | S) - \mathcal{E}_{\mathbf{X}}(S)$ , which we refer to as *oversampled sketchy ID (OSID)*.

To fill in a critical missing piece in the family of existing methods in Table 1 that leverage adaptiveness and randomness, in this work, we introduce **robust blockwise random pivoting (RBRP, Algorithm 4.1)**—an ID algorithm that is  $O(ndk)$ -time, parallelizable, error-revealing, and exact-ID-revealing, with comparable skeleton complexities to the nearly optimal random pivoting [5] in practice.

In particular, the plain blockwise random pivoting (*e.g.*, an extension of the blocked RPC-cholesky algorithm introduced in [5, Algorithm 2.2]) tends to suffer from unnecessarily large skeleton complexity (*cf.* Figure 1 (left)) under adversarial inputs (*e.g.*, Example 4.1) due to the lack of local adaptiveness within each block. As a remedy, RBRP leverages *robust blockwise filtering* (Remark 4.1)—applying CPQR to every small sampled block locally and discarding the potentially redundant points through a truncation on the relative residual of the CPQR. By choosing a reasonable block size, such robust blockwise filtering effectively resolves the inefficiency in skeleton complexity encountered by the plain blockwise random pivoting (*cf.* Figure 1 (right)), with negligible additional cost.

---

<sup>2</sup>It is worth mentioning that practical adaptive algorithms with “approximately” error-revealing properties are currently in active development.

Table 1: Summary of performance for skeleton selection methods that leverage adaptiveness and/or randomness. Recall from Equation (3) that  $\eta_r \triangleq \|\mathbf{X} - \mathbf{X}_{\langle r} \|^2_F / \|\mathbf{X}\|_F^2$ . The skeleton complexities in  $(\cdot)^*$  are conjectured based on extensive empirical evidence and intuitive rationale but without formal proofs. In the ‘‘Dominant Cost’’ column (*i.e.*, showing both the asymptotic complexity and parallelizability), ‘‘m-v’’ stands for matrix-vector multiplications, which are significantly less efficient than ‘‘m-m’’—matrix-matrix multiplications—due to the lack of parallelizability [19].

Skeleton Selection	Skeleton Complexity	Dominant Cost	Error-revealing	ID-revealing
Greedy pivoting/CPQR ([18, Section 5.4.2])	$k \geq (1 - (1 + \epsilon)\eta_r)n$	$O(ndk)$ m-v	<b>Yes</b>	<b>Exact</b>
Squared-norm sampling (Proposition 2.1 [13])	$k \geq \frac{r-1}{\epsilon\eta_r} + \frac{1}{\epsilon}$	$O(nd)$ <b>m-m</b>	No	Non
Random pivoting (Algorithm 3.1 [5])	$k \geq k_{\text{RP}} = \frac{r}{\epsilon} + r \min \left\{ \log \left( \frac{1}{\epsilon\eta_r} \right), 1 + \log \left( \frac{2r}{\epsilon} \right) \right\}$	$O(ndk)$ m-v	<b>Yes</b>	<b>Exact</b>
Sketchy pivoting (Algorithm 3.3 [15, 45])	$(k \gtrsim k_{\text{RP}})^*$	$O(ndk)$ <b>m-m</b>	No	Inexact
<b>RBRP</b> (this paper) (Algorithm 4.1)	$(k \gtrsim k_{\text{RP}})^*$	$O(ndk)$ <b>m-m</b>	<b>Yes</b>	<b>Exact</b>

### 1.3 Notations and Roadmap

For any fixed data matrix  $\mathbf{X} \in \mathbb{R}^{n \times d}$ , let  $\mathbf{X} = \mathbf{U}\mathbf{\Sigma}\mathbf{V}^\top = \sum_{i=1}^{\min(n,d)} \sigma_i \mathbf{u}_i \mathbf{v}_i^\top$  be the singular value decomposition of  $\mathbf{X}$  with  $\sigma_1 \geq \dots \geq \sigma_{\min(n,d)} \geq 0$ . Given any  $r \in [\min(n, d)]$ , we denote  $\mathbf{U}_r = [\mathbf{u}_1, \dots, \mathbf{u}_r]$ ,  $\mathbf{\Sigma}_r = \text{diag}(\sigma_1, \dots, \sigma_r)$ ,  $\mathbf{V}_r = [\mathbf{v}_1, \dots, \mathbf{v}_r]$  such that  $\mathbf{X}_{\langle r} = \mathbf{U}_r \mathbf{\Sigma}_r \mathbf{V}_r^\top$ .

We follow the MATLAB notation for vector and matrix indexing throughout this work. For any  $n \in \mathbb{N}$ , let  $[n] = \{1, \dots, n\}$  and  $\Delta_n = \{\mathbf{p} \in [0, 1]^n \mid \|\mathbf{p}\|_1 = 1\}$  be the probability simplex of dimension  $n$ . Also, let  $\mathfrak{S}_n$  be the set of all permutations of  $[n]$ . For any distribution  $\mathbf{p} \in \Delta_n$  and  $k \in \mathbb{N}$ ,  $\mathbf{p}^k$  represents the joint distribution over  $\Delta_n^k = \Delta_n \times \dots \times \Delta_n$  such that  $S = \{s_j \sim \mathbf{p}\}_{j \in [k]} \sim \mathbf{p}^k$  is a set of  $k$  *i.i.d.* samples. For any  $n \in \mathbb{N}$ , let  $\mathbf{e}_i$  ( $i \in [n]$ ) be the  $i$ -th canonical base of  $\mathbb{R}^n$ . For any  $m \in \mathbb{N}$ , let  $\mathbf{1}_m \in \mathbb{R}^m$  and  $\mathbf{0}_m \in \mathbb{R}^m$  be the vector with all entries equal to one and zero, respectively.

As a brief roadmap, we review the adaptiveness-only (greedy pivoting) and randomness-only (sampling) skeleton selection algorithms in Section 2, along with the two different combinations of adaptiveness and randomness (random and sketchy pivoting) in Section 3. Then, we introduce the RBRP algorithm formally in Section 4. In Section 5, we discuss the efficient construction of interpolation matrix for exact- and inexact-ID-revealing algorithms. Finally in Section 6, we present numerical experiments to demonstrate the strong empirical performance of RBRP in various settings. The code for numerical experiments is available at [https://github.com/dyjdongyijun/Robust\\_Blockwise\\_Random\\_Pivoting](https://github.com/dyjdongyijun/Robust_Blockwise_Random_Pivoting).

## 2 Adaptiveness vs. Randomness

### 2.1 Adaptiveness via Greedy Squared-norm Pivoting

Greedy pivoting is a classical way of incorporating adaptiveness in skeleton selection [20, 40, 45]. Column pivoted QR (CPQR) [18, Section 5.4.2] is one of the most commonly used greedy pivoting methods. The pivoting strategy and adaptive update are two key components that characterize a greedy pivoting method. In particular, CPQR involves greedy squared-norm pivoting and adaptive QR updates as synopsized below.

Starting with  $\mathbf{X}^{(0)} \leftarrow \mathbf{X}$ , given a(n) (active) data (sub)matrix  $\mathbf{X}^{(t)} \in \mathbb{R}^{n \times d}$  with at most  $n - t$  nonzero rows, CPQR on  $\mathbf{X}^\top$  greedily pivots the row in  $\mathbf{X}^{(t)}$  with the maximum  $\ell_2$ -norm (i.e., squared-norm pivoting):

$$s_{t+1} \leftarrow \operatorname{argmax}_{i \in [n]} \|\mathbf{X}^{(t)}(i, :)\|_2^2 \quad (4)$$

and adaptively updates the active submatrix by projecting it onto the orthogonal complement of the selected skeleton<sup>3</sup>:

$$\mathbf{X}^{(t+1)} \leftarrow \mathbf{X}^{(t)} - \mathbf{X}^{(t)} \frac{\mathbf{X}^{(t)}(s_{t+1}, :)\top \mathbf{X}^{(t)}(s_{t+1}, :)}{\|\mathbf{X}^{(t)}(s_{t+1}, :)\|_2^2}. \quad (5)$$

The (weak) rank-revealing property of CPQR [20, Theorem 7.2] implies that the first  $k$  pivots  $S = \{s_1, \dots, s_k\}$  form a reasonable skeleton subset with

$$\mathcal{E}_{\mathbf{X}}(S) \leq 4^k (n - k) \|\mathbf{X} - \mathbf{X}_{\langle k \rangle}\|_F^2. \quad (6)$$

The exponential dependence on  $k$  in Equation (6) is tight under adversarial inputs (e.g., Kahan matrices [25][20, Example 1]). In the worst case, CPQR can take almost all of the  $n$  points as skeletons before finding a  $(r, \epsilon)$ -ID. Concretely, [5, Theorem 4.1] implies that for CPQR,

$$\mathcal{E}_{\mathbf{X}}(S) \leq \frac{1}{\eta_r} \cdot \left(1 - \frac{k}{n}\right) \|\mathbf{X} - \mathbf{X}_{\langle r \rangle}\|_F^2. \quad (7)$$

That is, CPQR provides an  $(r, \epsilon)$ -ID when  $k \geq (1 - (1 + \epsilon)\eta_r)n$ . Moreover, for any  $|S| = k \leq \min(1 - (1 + \epsilon)\eta_r, \eta_r)n - 1$ , there exists an  $\mathbf{X}$  where CPQR fails to form an  $(r, \epsilon)$ -ID.

**Remark 2.1** (Greedy squared-norm pivoting is vulnerable but empirically successful). *The vulnerability to adversaries is a common and critical drawback of squared-norm pivoting in CPQR (and greedy pivoting methods in general). Nevertheless, it has been widely observed and conjectured that such adversarial inputs are extremely scarce in practice [42]. Therefore, CPQR serves as a good skeleton selection method for most data matrices empirically [15, 45].*

**Remark 2.2** (CPQR is inherently sequential but error-revealing). *From the computational efficiency perspective, a major drawback of CPQR is that the adaptive updates are inherently sequential (i.e., only half of the computation is cast in terms of matrix-matrix multiplication*

<sup>3</sup>For illustration, we consider the exact arithmetic here and express the QR update as a Gram-Schmidt process, whereas, in practice, QR updates are usually conducted via Householder reflection [18, Section 5.1.2] for numerical stability.

in the best-known algorithm that underlies LAPACK’s routine *geqp3* [36]). As a result, CPQR tends to be observably slower than simple alternatives with the same asymptotic complexity like Gaussian elimination with partial pivoting [18, Section 3.4]—another common greedy pivoting method that retains parallelizability at a cost of the rank-revealing guarantee.

Nevertheless, the adaptive nature grants CPQR an appealing bonus—the error-revealing ability. Specifically, it is known that the skeletonization error of CPQR, i.e.,  $\mathcal{E}_{\mathbf{X}}(S) = \|\mathbf{X}^{(S)}\|_F^2$ , can be downdated efficiently at the end of each update.

## 2.2 Randomness via Squared-norm Sampling

Sampling is a widely used approach for random skeleton selection (also referred to as column subset selection, e.g., in [8, 11]). To identify a nearly optimal (smallest possible) skeleton subset  $S$  for a  $(r, \epsilon)$ -ID, the intuitive goal is to construct a distribution  $\mathbf{p} \in \Delta_n$  over the  $n$  data points  $\{\mathbf{x}_i\}_{i \in [n]}$  that weights each  $\mathbf{x}_i$  according to its relative “importance”.

Analogous to the squared-norm pivoting in CPQR (Equation (4), Remark 2.1), sampling according to the squared-norm distribution is a natural choice for such “importance” sampling. Concretely, adapting results from [13] and [5, Theorem 4.2] leads to the following expected skeleton complexity for squared-norm sampling.

**Proposition 2.1** (Squared-norm sampling). *Consider a size- $k$  skeleton subset  $S = \{s_1, \dots, s_k\}$  where each  $s_j \in S$  is sampled from the squared-norm distribution  $s_j \sim \mathbf{p} = (p_1, \dots, p_n)$ ,  $p_i = \frac{\|\mathbf{x}_i\|_2^2}{\|\mathbf{X}\|_F^2}$  independently with replacement. Then*

$$\mathbb{E}_{S \sim \mathbf{p}^k} [\mathcal{E}_{\mathbf{X}}(S)] \leq \left(1 + \frac{r-1}{k\eta_r} + \frac{1}{k}\right) \|\mathbf{X} - \mathbf{X}_{\langle r \rangle}\|_F^2.$$

That is, squared-norm sampling provides a  $(r, \epsilon)$ -ID when  $k \geq \frac{r-1}{\epsilon\eta_r} + \frac{1}{\epsilon}$ .

Compared to the skeleton complexity guarantee of squared-norm pivoting (CPQR) in Equation (7), the squared-norm sampling in Proposition 2.1 provides a potentially weaker guarantee in expectation (instead of worst-case) but brings a better skeleton complexity that scales proportionally to  $r$  (instead of  $n$ ).

Despite the improved skeleton complexity in expectation compared to CPQR, like CPQR (Remark 2.1), squared-norm sampling can also be vulnerable to adversarial inputs by selecting redundant skeletons with higher probabilities. Such potential inefficiency can be reflected by the linear dependence of the skeleton complexity  $k \geq \frac{r-1}{\epsilon\eta_r} + \frac{1}{\epsilon}$  on  $\frac{r}{\eta_r}$ , as instantiated in Example 2.1.

**Example 2.1** (Adversarial input for squared-norm sampling). *For  $n \in \mathbb{N}$  divisible by  $k \in \mathbb{N}$ ,  $r \in \mathbb{N}$  such that  $k = (1 + \beta)r < n$  for some  $\beta \in \mathbb{N}$ , letting  $\alpha_i = \sqrt{\alpha} \gg \beta \geq 1$  for all  $1 \leq i \leq r$ , and  $\alpha_i = 1$  for all  $r+1 \leq i \leq k$ , we consider the following data matrix*

$$\mathbf{X}^\top = [\alpha_1 \mathbf{e}_1 \mathbf{I}_{n/k}^\top, \dots, \alpha_r \mathbf{e}_r \mathbf{I}_{n/k}^\top, \alpha_{r+1} \mathbf{e}_{r+1} \mathbf{I}_{n/k}^\top, \dots, \alpha_k \mathbf{e}_k \mathbf{I}_{n/k}^\top] \in \mathbb{R}^{d \times n}$$

with SVD

$$\mathbf{X} = \underbrace{\begin{bmatrix} \sqrt{\frac{k}{n}}\mathbf{I}_{n/k} & \cdots & \mathbf{0}_{n/k} \\ \vdots & \ddots & \vdots \\ \mathbf{0}_{n/k} & \cdots & \sqrt{\frac{k}{n}}\mathbf{I}_{n/k} \end{bmatrix}}_{\mathbf{U} \in \mathbb{R}^{n \times k}} \underbrace{\begin{bmatrix} \sqrt{\frac{n}{k}}\alpha_1 & & \\ & \ddots & \\ & & \sqrt{\frac{n}{k}}\alpha_k \end{bmatrix}}_{\mathbf{\Sigma} \in \mathbb{R}^{k \times k}} \underbrace{\begin{bmatrix} \mathbf{e}_1^\top \\ \vdots \\ \mathbf{e}_k^\top \end{bmatrix}}_{\mathbf{V}^\top \in \mathbb{R}^{k \times d}}.$$

Observe that a skeleton subset of size  $k$  with the  $k$  scaled canonical bases  $\{\alpha_i \mathbf{e}_i | i \in [k]\}$  is sufficient to form an ID that exactly recovers  $\mathbf{X}$ . That is, the uniform distribution over the  $k$  scaled canonical bases is preferred.

However, with  $\alpha \gg 1$ , the squared-norm distribution is heavily skewed to those rows in  $\mathbf{X}$  pointing toward  $\{\mathbf{e}_i | 1 \leq i \leq r\}$ , which leads to redundant samples along those directions:

$$p_i = \begin{cases} \frac{\alpha}{\alpha r + k - r} = \frac{\alpha}{(\alpha + \beta)r} & \forall 1 \leq i \leq r \\ \frac{1}{\alpha r + k - r} = \frac{1}{(\alpha + \beta)r} & \forall r + 1 \leq i \leq k \end{cases}.$$

Such inefficiency is well reflected in the skeleton complexity  $k \geq \frac{r-1}{\epsilon \eta_r} + \frac{1}{\epsilon}$  through a small  $\eta_r$ :

$$\eta_r = \frac{k - r}{\alpha r + k - r} = \frac{\beta}{\alpha + \beta} \ll 1.$$

For example, with  $\beta = 1$  and  $\alpha \gg k$ , the squared-norm sampling suffers from a skeleton complexity  $\frac{k}{\epsilon} + \frac{\alpha(r-1)-r}{\epsilon} \gg k$  far greater than necessary.

It is worth highlighting that adaptiveness is an effective remedy for such inefficiency of squared-norm sampling. For instance, after picking  $\alpha_i \mathbf{e}_i$  as the first skeleton, the adaptive update (e.g., Equation (5)) eliminates the remaining  $\frac{n}{k} - 1$  rows of  $\mathbf{X}$  in the  $\mathbf{e}_i$  direction and therefore helps exclude the possible redundant samples.

As well-studied alternatives to squared-norm sampling, determinantal point process (DPP sampling) [2, 10] and leverage score sampling [29] provide better skeleton complexity guarantees but with higher cost of constructing the corresponding distributions as a trade-off.

For example, the  $k$ -DPP sampling [27] is known for its *nearly optimal* skeleton complexity in expectation [2, 5, 21]:

$$k = |S| \geq \frac{r}{\epsilon} + r - 1 \Rightarrow \mathbb{E}_{S \sim k\text{-DPP}(\mathbf{X})} [\mathcal{E}_{\mathbf{X}}(S)] \leq (1 + \epsilon) \|\mathbf{X} - \mathbf{X}_{\langle r \rangle}\|_F^2. \quad (8)$$

As a trade-off, the classical SVD-based algorithm for  $k$ -DPP( $\mathbf{X}$ ) [23] takes  $O(nd^2)$  to construct the distribution and  $O(nk^2)$  to draw  $k$  samples.

In contrast to sampling from sophisticated distributions, uniform sampling works well for incoherent matrices (whose singular vectors distribute evenly along all canonical bases) but easily fails on coherent ones [7]. Although an in-depth comparison of different sampling methods is beyond the scope of this work, we refer the interested reader to the following enlightening references: [5, 7, 10, 13].



### 3 Combining Adaptiveness and Randomness

We recall that the vulnerability of greedy pivoting (Remark 2.1) comes from the scarce adversarial inputs which can be negligible in expectation under randomization. Meanwhile, the vulnerability of squared-norm sampling (Example 2.1) can be effectively circumvented by incorporating adaptive updates. Therefore, a natural question is *how to combine adaptiveness and randomness effectively for better skeleton selection*. In this section, we review two existing ideas that involve both adaptiveness and randomness in different ways, while comparing their respective advantages and drawbacks.

#### 3.1 Random Pivoting

Random pivoting [1, 5, 12, 13] is arguably the most intuitive skeleton selection method that combines adaptiveness and randomness. It can be simply described as “replacing the greedy squared-norm pivoting in CPQR with squared-norm sampling” or “adaptively updating the dataset via QR after each step of squared-norm sampling”, as formalized in Algorithm 3.1.

---

#### Algorithm 3.1 Sequential random pivoting (SRP)

---

**Require:** (a) Data matrix  $\mathbf{X} = [\mathbf{x}_1, \dots, \mathbf{x}_n]^\top \in \mathbb{R}^{n \times d}$ , (b) Relative error tolerance  $\tau = (1 + \epsilon) \eta_r \in (0, 1)$  (or target rank  $k \in \mathbb{N}$ ),

**Ensure:** (a) Skeleton indices  $S = \{s_1, \dots, s_k\} \subset [n]$ , (b)  $\mathbf{L} \in \mathbb{R}^{n \times k}$ , (c)  $\boldsymbol{\pi} \in \mathfrak{S}_n$

- 1:  $\mathbf{L}^{(0)} \leftarrow \mathbf{0}_{n \times 0}$ ,  $\mathbf{Q}^{(0)} \leftarrow \mathbf{0}_{d \times 0}$ ,  $\boldsymbol{\pi} \leftarrow [1, \dots, n]$ ,  $S \leftarrow \emptyset$ ,  $t = 0$
- 2:  $\mathbf{d}^{(0)} \in \mathbb{R}_{\geq 0}^n$  with  $\mathbf{d}^{(0)}(i) = \|\mathbf{x}_i\|_2^2 \forall i \in [n]$   $\triangleright O(nd)$
- 3: **while**  $\|\mathbf{d}^{(t)}\|_1 < \tau \|\mathbf{d}^{(0)}\|_1$  (or  $|S| < k$ ) **do**
- 4:    $t \leftarrow t + 1$
- 5:    $s_t \sim \mathbf{d}^{(t-1)} / \|\mathbf{d}^{(t-1)}\|_1$
- 6:    $S \leftarrow S \cup \{s_t\}$ ,  $\boldsymbol{\pi} \leftarrow \text{swap}(\boldsymbol{\pi}, t, s_t)$   $\triangleright \boldsymbol{\pi}(1:t)$  consists of  $S$
- 7:    $\mathbf{a}^{(t)} \leftarrow \mathbf{0}_n$ ,  $\boldsymbol{\pi}_a \leftarrow \boldsymbol{\pi}(t:n)$   $\triangleright$  “a” for active
- 8:    $\mathbf{v} \leftarrow \mathbf{x}_{s_t} - \mathbf{Q}^{(t-1)} \left( (\mathbf{Q}^{(t-1)})^\top \mathbf{x}_{s_t} \right) \in \mathbb{R}^d$   $\triangleright O(dt)$
- 9:    $\mathbf{Q}^{(t)} \leftarrow [\mathbf{Q}^{(t-1)}, \mathbf{v} / \|\mathbf{v}\|_2] \in \mathbb{R}^{d \times t}$   $\triangleright O(d)$
- 10:    $\mathbf{a}^{(t)}(\boldsymbol{\pi}_a) \leftarrow \mathbf{X}(\boldsymbol{\pi}_a, :) \mathbf{v}$   $\triangleright O(nd)$
- 11:    $\mathbf{L}^{(t)} \leftarrow [\mathbf{L}^{(t-1)}, \mathbf{a}^{(t)} / \sqrt{\mathbf{a}^{(t)}(s_t)}]$   $\triangleright \mathbf{a}^{(t)}(s_t) = \mathbf{d}^{(t-1)}(s_t)$
- 12:    $\mathbf{d}^{(t)}(i) \leftarrow 0 \forall i \in S$ ,  $\mathbf{d}^{(t)}(i) \leftarrow \mathbf{d}^{(t-1)}(i) - \frac{(\mathbf{a}^{(t)}(i))^2}{\mathbf{a}^{(t)}(s_t)} \forall i \notin S$   $\triangleright O(n)$
- 13:  $k \leftarrow |S|$ ,  $\mathbf{L} \leftarrow \mathbf{L}^{(t)}$

---

Algorithm 3.1 has an asymptotic complexity of  $O(ndk + dk^2)$ , with  $k$  inherently sequential passes through  $\mathbf{X}$  (or its submatrices), while the storage of  $\mathbf{L}^{(t)}$  and  $\mathbf{Q}^{(t)}$  requires  $O(nk)$  and  $O(dk)$  memory, respectively. Meanwhile, analogous to greedy pivoting (Remark 2.2), Algorithm 3.1 is error-revealing thanks to its adaptive nature.

The idea of random pivoting in Algorithm 3.1 is ubiquitous in various related problems, *e.g.*, the combination of volume sampling and adaptive sampling for low-rank approximation [12], the Randomly Pivoted Cholesky (RPCholesky) [5] for kernel column Nyström approximation [30, 19.2], and the  $D^2$ -sampling for k-means++ clustering [1].

Specifically, applying RPCholesky [5, Algorithm 2.1] to the kernel matrix  $\mathbf{X}\mathbf{X}^\top \in \mathbb{R}^{n \times n}$  can be reformulated as Algorithm 3.2, which is equivalent to Algorithm 3.1 in the exact arithmetic (Remark 3.1). Compared to Algorithm 3.1, the skeleton selection stage of Algorithm 3.2 has an asymptotic complexity of  $O(ndk + nk^2)$  (cf.  $O(ndk + dk^2)$  for Algorithm 3.1), while only requires  $O(nk)$  memory for the storage of  $\mathbf{L}^{(t)}$ .

---

**Algorithm 3.2** RPCholesky [5, Algorithm 2.1]

---

```

1:  $\mathbf{L}^{(0)} \leftarrow \mathbf{0}_{n \times 0}$ ,  $\boldsymbol{\pi} \leftarrow [1, \dots, n]$ ,  $S \leftarrow \emptyset$ ,  $t = 0$ 
2:  $\mathbf{d}^{(0)} \in \mathbb{R}_{\geq 0}^n$  with  $\mathbf{d}^{(0)}(i) = \|\mathbf{x}_i\|_2^2 \forall i \in [n]$   $\triangleright O(nd)$ 
3: while  $\|\mathbf{d}^{(t)}\|_1 < \tau \|\mathbf{d}^{(0)}\|_1$  (or  $|S| < k$ ) do
4:    $t \leftarrow t + 1$ 
5:    $s_t \sim \mathbf{d}^{(t-1)} / \|\mathbf{d}^{(t-1)}\|_1$ 
6:    $S \leftarrow S \cup \{s_t\}$ ,  $\boldsymbol{\pi} \leftarrow \text{swap}(\boldsymbol{\pi}, t, s_t)$   $\triangleright \boldsymbol{\pi}(1:t)$  consists of  $S$ 
7:    $\mathbf{a}^{(t)} \leftarrow \mathbf{0}_n$ ,  $\boldsymbol{\pi}_a \leftarrow \boldsymbol{\pi}(t:n)$   $\triangleright$  “a” for active
8:    $\mathbf{a}^{(t)}(\boldsymbol{\pi}_a) \leftarrow \mathbf{X}(\boldsymbol{\pi}_a, :) \mathbf{x}_{s_t} - \mathbf{L}^{(t-1)}(\boldsymbol{\pi}_a, 1:t-1) \mathbf{L}^{(t-1)}(s_t, 1:t-1)^\top$   $\triangleright O(nd + nt)$ 
9:    $\mathbf{L}^{(t)} \leftarrow \left[ \mathbf{L}^{(t-1)}, \mathbf{a}^{(t)} / \sqrt{\mathbf{a}^{(t)}(s_t)} \right]$   $\triangleright \mathbf{a}^{(t)}(s_t) = \mathbf{d}^{(t-1)}(s_t)$ 
10:   $\mathbf{d}^{(t)}(i) \leftarrow 0 \forall i \in S$ ,  $\mathbf{d}^{(t)}(i) \leftarrow \mathbf{d}^{(t-1)}(i) - \frac{(\mathbf{a}^{(t)}(i))^2}{\mathbf{a}^{(t)}(s_t)} \forall i \notin S$   $\triangleright O(n)$ 

```

---

**Remark 3.1** (Relation between QR with sequential random pivoting and RPCholesky). *Sequential random pivoting (Algorithm 3.1) on  $\mathbf{X}$  is equivalent to RPCholesky (Algorithm 3.2 [5, Algorithm 2.1]) on  $\mathbf{X}\mathbf{X}^\top$  in the exact arithmetic.*

*Rationale for Remark 3.1.* To show the equivalence in the exact arithmetic, it is sufficient to observe that Algorithms 3.1 and 3.2 yield the same  $\mathbf{a}^{(t)}$  and  $\mathbf{d}^{(t)}$  in each iteration  $t = 1, 2, \dots$ .

By induction, when  $t = 1$ , both Algorithms 3.1 and 3.2 lead to  $\mathbf{a}^{(1)} = \mathbf{X}\mathbf{x}_{s_1}$  and

$$\mathbf{d}^{(1)}(i) = \|\mathbf{x}_i\|_2^2 - \frac{(\mathbf{x}_i^\top \mathbf{x}_{s_1})^2}{\|\mathbf{x}_{s_1}\|_2^2} = \left\| \left( \mathbf{I}_d - \mathbf{Q}^{(1)} (\mathbf{Q}^{(1)})^\top \right) \mathbf{x}_i \right\|_2^2 \quad \forall i \in [n] \setminus \{s_1\},$$

while  $\mathbf{d}^{(1)}(s_1) = 0$ . We also observe that  $\mathbf{L}^{(1)} = \mathbf{X}\mathbf{Q}^{(1)}$  since  $\mathbf{a}^{(1)}(s_1) = \|\mathbf{x}_{s_1}\|_2^2$ .

Suppose that in the  $(t-1)$ -th iteration, Algorithms 3.1 and 3.2 produce equivalent  $\mathbf{a}^{(t-1)}$  and  $\mathbf{d}^{(t-1)}$  under the exact arithmetic, while  $\mathbf{d}^{(t-1)}(i) = \left\| \left( \mathbf{I}_d - \mathbf{Q}^{(t-1)} (\mathbf{Q}^{(t-1)})^\top \right) \mathbf{x}_i \right\|_2^2$  for all  $i \in [n]$  and  $\mathbf{L}^{(t-1)} = \mathbf{X}\mathbf{Q}^{(t-1)}$ .

Then in the  $t$ -th iteration, both Algorithms 3.1 and 3.2 compute

$$\mathbf{a}^{(t)} = \mathbf{X}\mathbf{x}_{s_t} - \mathbf{X}\mathbf{Q}^{(t-1)} (\mathbf{Q}^{(t-1)})^\top \mathbf{x}_{s_t} = \mathbf{X} \left( \mathbf{I}_d - \mathbf{Q}^{(t-1)} (\mathbf{Q}^{(t-1)})^\top \right) \mathbf{x}_{s_t},$$

$\mathbf{L}^{(t)} = \mathbf{X}\mathbf{Q}^{(t)}$ , and for all  $i \in [n]$ ,

$$\begin{aligned} \mathbf{d}^{(t)}(i) &= \left\| \left( \mathbf{I}_d - \mathbf{Q}^{(t-1)} (\mathbf{Q}^{(t-1)})^\top \right) \mathbf{x}_i \right\|_2^2 - \frac{\left( \mathbf{x}_i^\top \left( \mathbf{I}_d - \mathbf{Q}^{(t-1)} (\mathbf{Q}^{(t-1)})^\top \right) \mathbf{x}_{s_t} \right)^2}{\mathbf{x}_{s_t}^\top \left( \mathbf{I}_d - \mathbf{Q}^{(t-1)} (\mathbf{Q}^{(t-1)})^\top \right) \mathbf{x}_{s_t}} \\ &= \left\| \left( \mathbf{I}_d - \mathbf{Q}^{(t)} (\mathbf{Q}^{(t)})^\top \right) \mathbf{x}_i \right\|_2^2. \end{aligned}$$

■

In light of the equivalence between Algorithms 3.1 and 3.2, [5, Theorem 3.1] provides the following skeleton complexity guarantee for sequential random pivoting.

**Proposition 3.1** (Sequential random pivoting). *For any  $\epsilon > 0$  and  $r \in [n]$ , the skeleton subset  $S$  selected by Algorithm 3.1 provides  $\mathbb{E}[\mathcal{E}_{\mathbf{X}}(S)] \leq (1 + \epsilon) \|\mathbf{X} - \mathbf{X}_{\langle r \rangle}\|_F^2$  (i.e., a  $(r, \epsilon)$ -ID in expectation) when<sup>4</sup>*

$$k = |S| \geq \frac{r}{\epsilon} + r \cdot \min \left\{ \log \left( \frac{1}{\epsilon \eta_r} \right), 1 + \log \left( \frac{2^r}{\epsilon} \right) \right\}.$$

From Proposition 3.1, we notice that sequential random pivoting almost matches the nearly optimal skeleton complexity guarantee of DPP (Equation (8)) up to some logarithmic factors  $\log \left( \frac{1}{\epsilon \eta_r} \right)$  on  $r$ . Further, the appealing skeleton complexity of random pivoting is empirically demonstrated in the form of RPCholesky for column Nyström approximation in [5].

Although random pivoting leverages the strength of both adaptiveness and randomness and achieves an appealing skeleton complexity with an affordable asymptotic complexity, the lack of parallelizability due to its sequential nature becomes a critical concern when considering empirical runtime.

**Remark 3.2** (Inefficiency of sequential updates). *Given a sequence of matrix operations, it is well known that an appropriate implementation using Level-3 BLAS, or matrix-matrix, operations will run more efficiently on modern processors than an optimal implementation using Level-2 or Level-1 BLAS [3]. This is largely due to the greater potential for the Level-3 BLAS to make more efficient use of memory caching in the processor. Notice that the computational bottleneck of Algorithm 3.1 with asymptotic complexity  $O(ndk)$  (or  $O(ndk)$ ) consists of  $k$  matrix-vector multiplications (Level-2 BLAS) with  $\mathbf{X}$ . This leads to the considerable slowdown of Algorithm 3.1 in practice.*

## 3.2 Sketchy Pivoting

Alternative to random pivoting, randomness can be combined with adaptiveness through randomized linear embedding (also known as sketching), which leads to the sketchy pivoting methods [15, 31, 45]. As given in Algorithm 3.3, the general framework of sketching pivoting [15, Algorithm 1] consists of two stages.

<sup>4</sup>Without strictly specifying, we generally assume that  $\epsilon > 0$  is reasonably small such that the  $(r, \epsilon)$ -ID is a non-trivial approximation, i.e.,  $\epsilon < \min \{1/\eta_r, 2^r\}$  such that both logarithmic terms are positive. Otherwise, the skeleton complexity guarantee still holds by replacing any negative logarithmic terms with zeros.

---

**Algorithm 3.3** Sketchy pivoting [15, 45] (SkLUPP/SkCPQR)

---

**Require:** (a)  $\mathbf{X} = [\mathbf{x}_1, \dots, \mathbf{x}_n]^\top \in \mathbb{R}^{n \times d}$ , (b) Target rank  $k \in \mathbb{N}$ , (c) Sample size  $l \geq k$ , (d) Pivoting strategy: LUPP/CPQR

**Ensure:** (a)  $S = \{s_1, \dots, s_k\} \subset [n]$ , (b)  $\mathbf{L} \in \mathbb{R}^{n \times k}$ , (c)  $\boldsymbol{\pi} \in \mathfrak{S}_n$

- 1: Draw a randomized linear embedding  $\boldsymbol{\Omega} \in \mathbb{R}^{d \times l}$
  - 2:  $\mathbf{Y} \leftarrow \mathbf{X}\boldsymbol{\Omega} \in \mathbb{R}^{n \times l}$   $\triangleright O(ndk)$
  - 3: **if** LUPP **then**
  - 4:      $\mathbf{L}, \sim, \boldsymbol{\pi} \leftarrow \text{lu}(\mathbf{Y}(:, 1:k), \text{“vector”})$  [15]  $\triangleright \mathbf{L} \in \mathbb{R}^{n \times k}, O(nk^2)$
  - 5: **else if** CPQR **then**
  - 6:      $\sim, \mathbf{L}^\top, \boldsymbol{\pi} \leftarrow \text{qr}(\mathbf{Y}(:, 1:k)^\top, \text{“econ”}, \text{“vector”})$  [45]  $\triangleright \mathbf{L} \in \mathbb{R}^{n \times k}, O(nk^2)$
  - 7:  $S \leftarrow \boldsymbol{\pi}(1:k)$
- 

In the first stage, *randomness is incorporated through sketching*, which serves two purposes.

- From the computational efficiency perspective, sketching reduces the data dimension from  $d$  to  $l = O(k)^5$ , while transferring the  $O(ndk)$  computational bottleneck from the sequential greedy pivoting to the (input-sparsity-time and) parallelizable matrix-matrix multiplications.
- From the skeleton complexity perspective, applying randomized embedding to the row space of  $\mathbf{X}$  via sketching improves the empirical robustness of the subsequent greedy pivoting [15, 42]. Intuitively, this is because the scarce adversarial inputs for greedy pivoting (Remark 2.1) are effectively negligible under randomization.

Common choices of randomized linear embeddings in the sketching stage include Gaussian embedding [24] (with asymptotic complexity  $O(ndk)$ ), subsampled randomized trigonometric transforms [4, 38, 43, 47] (with asymptotic complexity  $O(nd \log(k))$ ), and sparse embeddings [6, 32, 33, 44] (with asymptotic complexity  $O(nd)$ ). We refer the interested readers to [22, 30, 46] for a general review of sketching.

In the second stage, *adaptiveness is utilized as greedy pivoting on the sketched sample matrix*  $\mathbf{Y} = \mathbf{X}\boldsymbol{\Omega} \in \mathbb{R}^{n \times l}$  to select skeletons. Both LUPP [18, Section 3.4] and CPQR [18, Section 5.4.2] on  $\mathbf{Y}$  cost  $O(nk^2)$  asymptotically, whereas LUPP is remarkably faster in practice due to its superior parallelizability [15]. Intuitively, applying greedy pivoting on the top of sketching can be viewed as an analog of the squared-norm sampling with a slightly different squared-norm-based distribution.

For example, for a Gaussian random matrix  $\boldsymbol{\Omega}$  with *i.i.d.* entries from  $\mathcal{N}(0, 1/l)$ , each row  $\mathbf{y}_i = \boldsymbol{\Omega}^\top \mathbf{x}_i$  of  $\mathbf{Y}$  is a Gaussian random vector with *i.i.d.* entries from  $\mathcal{N}(\mathbf{0}, \|\mathbf{x}_i\|_2^2 \mathbf{I}_l)$ <sup>6</sup>. When applying greedy squared-norm pivoting (CPQR) in the second stage, the first pivot is selected according to  $s_1 \leftarrow \operatorname{argmax}_{i \in [n]} \|\mathbf{x}_i\|_2^2 Z_i$  where every  $Z_i = \sum_{j=1}^l Y_{ij}^2$  is a  $\chi_l^2$  random variable but  $\{Z_i \mid i \in [n]\}$  are dependent. The intuition behind sketchy pivoting is similar to random pivoting, but the randomness arises from the random variables  $Z_i$ , instead of sampling, which

---

<sup>5</sup>For applications like low-rank approximations and skeleton selection, a small constant oversampling like  $k+5 \leq l \leq k+10$  is usually sufficient in practice.

<sup>6</sup>It is worth highlighting that although rows of  $\mathbf{Y}$  consist of *i.i.d.* entries, entries in each column of  $\mathbf{Y}$  are dependent. In particular, for all  $j \in [l]$ ,  $\operatorname{Cov}(\mathbf{Y}(:, j)) = \mathbf{X}\mathbf{D}^{-1}\mathbf{X}^\top$  where  $\mathbf{D} = \operatorname{diag}(\|\mathbf{x}_1\|_2^2, \dots, \|\mathbf{x}_n\|_2^2)$ .

leads to the following conjecture.

**Conjecture 3.2.** *There exists a distribution  $P : \mathbb{R} \rightarrow [0, 1]$  satisfying the universality assumptions (e.g.,  $P$  is symmetric and zero-mean with bounded variance<sup>7</sup>) such that the following holds. For the  $l$  independent random vectors  $\left\{ \mathbf{Y}(:, j) = [Y_{1j}, \dots, Y_{nj}]^\top \mid j \in [l] \right\}$  such that*

$$Y_{ij} \sim P, \quad \mathbb{E}[\mathbf{Y}(:, j)] = \mathbf{0}, \quad \text{Cov}(\mathbf{Y}(:, j)) = \mathbf{X}\mathbf{D}^{-1}\mathbf{X}^\top \quad \forall j \in [l],$$

where  $\mathbf{D} = \text{diag}(\|\mathbf{x}_1\|_2^2, \dots, \|\mathbf{x}_n\|_2^2)$ , the induced discrete random variable

$$s \leftarrow \underset{i \in [n]}{\text{argmax}} \|\mathbf{x}_i\|_2^2 Z_i, \quad Z_i = \sum_{j=1}^l Y_{ij}^2 \quad \forall i \in [n]$$

follows the squared-norm distribution  $p(s) \approx \|\mathbf{x}_s\|_2^2 / \|\mathbf{X}\|_F^2$ .

In the extreme scenarios, when the variance of  $\{Z_i\}_{i \in [n]}$  is negligible in comparison to the squared norms  $\{\|\mathbf{x}_i\|_2^2\}_{i \in [n]}$ , sketchy pivoting behaves similarly to greedy pivoting. Meanwhile, when the variance of  $\{Z_i\}_{i \in [n]}$  is much larger than differences among the squared norms, sketchy pivoting tends to behave like uniform sampling. Therefore intuitively, there exist some appropriate choices of variance interpolating the two extreme cases such that sketchy pivoting mimics the behavior of squared-norm sampling.

Suppose Conjecture 3.2 holds for some distribution  $P$ , then sketchy pivoting (e.g., SkCPQR in Algorithm 3.3) with a randomized linear embedding  $\Omega$  consisting of *i.i.d.* entries drawn from  $P$  is equivalent to sequential random pivoting (Algorithm 3.1), which enjoys the nearly optimal skeleton complexity guarantee in Proposition 3.1.

In practice, sketchy pivoting (Algorithm 3.3) with Gaussian embedding provides high-quality skeleton selection with comparable error  $\mathcal{E}_X(S)$  to random pivoting (Algorithm 3.1, cf. Figure 1), but much more efficiently thanks to the parallelizability of sketching [15]. However, as a major empirical limitation, sketchy pivoting is not error-revealing and requires prior knowledge of the target rank  $k$ .

## 4 Robust Blockwise Random Pivoting

In light of the existing skeleton selection methods summarized in Table 1 that leverage/combine randomness and adaptiveness, a *parallelizable, error-revealing, and exact-ID-revealing* skeleton selection algorithm that attains similar skeleton and asymptotic complexities as the sequential random pivoting is a desirable missing piece.

Blockwise random pivoting is a natural extension of its sequential variation Algorithm 3.1 that consists of matrix-matrix multiplications and is therefore parallelizable. In the kernel formulation (with an input kernel matrix  $\mathbf{X}\mathbf{X}^\top$ ), [5, Algorithm 2.2] introduced a blocked version of RPCholesky that can be generalized as blockwise random pivoting (BRP—Algorithm 4.1 with  $\tau_b = 0$ ). However, for a large block size  $b \in \mathbb{N}$  that improves parallelizability, such plain BRP

<sup>7</sup>[34, Model 2.1, Theorem 9.1] implies that when  $P$  is symmetric with mean zero and variance bounded, a random matrix  $\Omega \in \mathbb{R}^{d \times l}$  ( $l \leq d$ ) with bounded *i.i.d.* entries from  $P$  serves as a randomized linear embedding.

can pick up to  $b$  times more skeletons than necessary due to the similar pitfall of squared-norm sampling instantiated in Example 2.1 (e.g., Figure 1). Moreover, in practice, the numerical instability issue tends to be exacerbated as the block size increases.

---

**Algorithm 4.1** Robust blockwise random pivoting (RBRP)

---

**Require:** (a)  $\mathbf{X} = [\mathbf{x}_1, \dots, \mathbf{x}_n]^\top \in \mathbb{R}^{n \times d}$ , (b)  $\tau = (1 + \epsilon) \eta_r \in (0, 1)$  (or  $k \in \mathbb{N}$ ), (c) Block size  $b \in \mathbb{N}$ , (d)  $\tau_b \in [0, 1]$ —Tolerance for blockwise filtering (we choose  $\tau_b = \frac{1}{b}$ )

**Ensure:** (a)  $S = \{s_1, \dots, s_k\} \subset [n]$ , (b)  $\mathbf{L} \in \mathbb{R}^{n \times k}$ , (c)  $\boldsymbol{\pi} \in \mathfrak{S}_n$

- 1:  $\mathbf{L}^{(0)} \leftarrow \mathbf{0}_{n \times 0}$ ,  $\mathbf{Q}^{(0)} \leftarrow \mathbf{0}_{d \times 0}$ ,  $\boldsymbol{\pi} \leftarrow [1, \dots, n]$ ,  $S \leftarrow \emptyset$ ,  $t = 0$
- 2:  $\mathbf{d}^{(0)} \in \mathbb{R}_{\geq 0}^n$  with  $\mathbf{d}^{(0)}(i) = \|\mathbf{x}_i\|_2^2 \forall i \in [n]$   $\triangleright O(nd)$
- 3: **while**  $\|\mathbf{d}^{(t)}\|_1 < \tau \|\mathbf{d}^{(0)}\|_1$  (or  $|S| < k$ ) **do**
- 4:    $t \leftarrow t + 1$ ,  $b \leftarrow \min(b, k - |S|)$
- 5:   Sample  $S_t = (s_{|S|+1}, \dots, s_{|S|+b}) \sim \mathbf{d}^{(t-1)} / \|\mathbf{d}^{(t-1)}\|_1$  without replacement  $\triangleright O(n)$
- 6:    $\mathbf{V} \leftarrow \mathbf{X}(S_t, :)^T - \mathbf{Q}^{(t-1)} \left( (\mathbf{Q}^{(t-1)})^\top \mathbf{X}(S_t, :)^T \right) \in \mathbb{R}^{d \times b}$   $\triangleright O(db|S|)$
- 7:    $\mathbf{Q}_V, \mathbf{R}_V, \boldsymbol{\pi}_V \leftarrow \text{qr}(\mathbf{V}, \text{“econ”}, \text{“vector”})$   $\triangleright \mathbf{Q}_V \in \mathbb{R}^{d \times b}, \mathbf{R}_V \in \mathbb{R}^{b \times b}, O(db^2)$
- 8:    $b' \leftarrow \max \{i \in [b] \mid \|\mathbf{R}_V(i : b, i : b)\|_F^2 \geq \tau_b \cdot \|\mathbf{R}_V\|_F^2\}$   $\triangleright O(b^2)$
- 9:    $S'_t \leftarrow S_t(\boldsymbol{\pi}_V(1 : b'))$ ,  $\mathbf{Q}'_V \leftarrow \mathbf{Q}_V(:, 1 : b')$
- 10:    $\mathbf{Q}^{(t)} \leftarrow [\mathbf{Q}^{(t-1)}, \mathbf{Q}'_V] \in \mathbb{R}^{d \times (|S|+b')}$
- 11:    $\boldsymbol{\pi} \leftarrow \text{swap}(\boldsymbol{\pi}, |S| + 1 : |S| + b', S'_t)$ ,  $\boldsymbol{\pi}_a \leftarrow \boldsymbol{\pi}(|S| + 1 : n)$
- 12:    $\widehat{\mathbf{L}}^{(t)} \leftarrow \mathbf{0}_{n \times b'}$
- 13:    $\widehat{\mathbf{L}}^{(t)}(\boldsymbol{\pi}_a, :) \leftarrow \mathbf{X}(\boldsymbol{\pi}_a, :) \mathbf{Q}_V$   $\triangleright$  for block triangular  $\mathbf{L}_1$  (Remark 5.1),  $O(ndb')$
- 14:    $S \leftarrow S \cup S'_t$
- 15:    $\mathbf{L}^{(t)} \leftarrow [\mathbf{L}^{(t-1)}, \widehat{\mathbf{L}}^{(t)}] \in \mathbb{R}^{n \times |S|}$
- 16:    $\mathbf{d}^{(t)}(i) \leftarrow 0 \forall i \in S$ ,  $\mathbf{d}^{(t)}(i) \leftarrow \mathbf{d}^{(t-1)}(i) - \|\widehat{\mathbf{L}}^{(t)}(i, :)\|_2^2 \forall i \notin S$   $\triangleright O(nb')$
- 17:  $k \leftarrow |S|$ ,  $\mathbf{L} \leftarrow \mathbf{L}^{(t)}$

---

To exemplify the pitfall of plain BRP, we present an adversarial input in Example 4.1 based on a tailored Gaussian mixture model (GMM).

**Example 4.1** (Pitfall of plain blockwise random pivoting). *For  $n, d, k \in \mathbb{N}$  such that  $n/k = m \in \mathbb{N}$ , we draw  $n$  points from a GMM with means  $\mathcal{C} = \{\boldsymbol{\mu}_j\}_{j \in [k]}$ , covariance  $\mathbf{I}_d$ , and cluster size  $m$ — $\mathcal{X} = \{\mathbf{x}_i \in \mathbb{R}^d\}_{i \in [n]} = \bigcup_{j=1}^k \mathcal{X}_j$  where*

$$\mathcal{X}_j = \{\mathbf{x}_{m(j-1)+\iota} = \boldsymbol{\mu}_j + \boldsymbol{\xi}_\iota \mid \boldsymbol{\mu}_j = 10j \cdot \mathbf{e}_j, \boldsymbol{\xi}_\iota \sim \mathcal{N}(\mathbf{0}_d, \mathbf{I}_d) \text{ i.i.d. } \forall \iota \in [m]\}.$$

*Consider a GMM data matrix  $\mathbf{X} = [\mathbf{x}_1, \dots, \mathbf{x}_n]^\top \in \mathbb{R}^{n \times d}$ . Since the means in  $\mathcal{C}$  have distinct norms whose discrepancies dominate the covariance  $\mathbf{I}_d$ ,  $\mathcal{X}$  can be partitioned into  $k$  clusters  $\{\mathcal{X}_j\}_{j \in [k]}$  each containing  $m$  points with distinct norms.*

*The best size- $k$  skeleton subset consists of exactly one point from each cluster  $\mathcal{X}_j$ , while multiple points from the same cluster are redundant. However, the plain blockwise adaptiveness (random (BRP)/greedy pivoting (BGP)) tends to pick multiple points from the same cluster. For instance, with block size  $b$ , BGP can pick up to  $\min(b, m)$  points in the same cluster. Similar inefficiency also appears in the BRP but is generally alleviated thanks to the randomness (Figure 1 (left)).*

To resolve the challenges illustrated by Example 4.1, we introduce a *robust blockwise random pivoting (RBRP)* algorithm—Algorithm 4.1—that empirically achieves comparable skeleton complexities as the sequential adaptive methods (SRP and CPQR), as demonstrated in Figure 1 (right), while exploiting the parallelizability of matrix-matrix multiplications.

**Remark 4.1** (Robust blockwise filtering). *The key step in Algorithm 4.1 that improves the robustness of BRP is the robust blockwise filtering with tolerance  $\tau_b \in [0, 1]$ —applying the truncated CPQR locally on the small residuals of the selected candidates  $\mathbf{V} \in \mathbb{R}^{d \times b}$ :*

$$\mathbf{V}(:, \pi_{\mathbf{V}}) = \mathbf{Q}_{\mathbf{V}} \mathbf{R}_{\mathbf{V}} \approx \mathbf{Q}_{\mathbf{V}}(:, 1:b') \mathbf{R}_{\mathbf{V}}(1:b', :)$$

where the relative truncation error is upper bounded by  $\tau_b$

$$\|\mathbf{V}(:, \pi_{\mathbf{V}}) - \mathbf{Q}_{\mathbf{V}}(:, 1:b') \mathbf{R}_{\mathbf{V}}(1:b', :)\|_F^2 = \|\mathbf{R}_{\mathbf{V}}(b'+1:b, b'+1:b)\|_F^2 < \tau_b \|\mathbf{V}\|_F^2.$$

With small constant block sizes, the robust blockwise filtering based on local CPQR can be computed with negligible additional cost  $O(db^2)$ , despite the sequential nature of CPQR.

In general, Algorithm 4.1 takes  $O(ndk + bdk^2)$  time asymptotically (with a slightly larger lower-order term, cf.  $O(ndk + dk^2)$  for the sequential version in Algorithm 3.1), where the dominant cost  $O(ndk)$  consists of  $k$  parallelizable passes through  $\mathbf{X}$ . Analogous to Algorithm 3.1, the storage of  $\mathbf{L}^{(t)}$  and  $\mathbf{Q}^{(t)}$  requires  $O(nk)$  and  $O(dk)$  memory, respectively. Meanwhile, the adaptiveness grants Algorithm 4.1 the blockwise error-revealing ability.

Table 2: Summary of abbreviations for the skeleton selection methods in the experiments.

Abbreviation	Skeleton selection method	Algorithm
CPQR	Sequential greedy pivoting	[18, Section 5.4.2]
SqNorm	Squared-norm sampling	Proposition 2.1 [13]
DPP	DPP sampling	[2, Equation 8][17, 27]
SRP	Sequential random pivoting	Algorithm 3.1 [5]
SkCPQR	Sketchy pivoting with CPQR	Algorithm 3.3 [45]
SkLUPP	Sketchy pivoting with LUPP	Algorithm 3.3 [15]
BGP	Blockwise greedy pivoting	Remark 4.2 with $\tau_b = 0$
BRP	Blockwise random pivoting	Algorithm 4.1 with $\tau_b = 0$
RBGP	Robust blockwise greedy pivoting	Remark 4.2 with $\tau_b = \frac{1}{b}$
<b>RBRP</b>	<b>Robust blockwise random pivoting</b>	<b>Algorithm 4.1 with <math>\tau_b = \frac{1}{b}</math></b>

**Remark 4.2** (Blockwise greedy pivoting). *For the completeness of comparison, in the experiments, we consider a variation of the (robust) blockwise random pivoting ((R)BRP)—(robust) blockwise greedy pivoting ((R)BGP). In Algorithm 4.1, (R)BGP replaces the sampling step,*

$$\text{sample } S_t = (s_{|S|+1}, \dots, s_{|S|+b}) \sim \mathbf{d}^{(t-1)} / \|\mathbf{d}^{(t-1)}\|_1 \text{ without replacement}$$

with the task of choosing points corresponding to the top- $b$  probabilities greedily:

$$\text{select } S_t = (s_{|S|+1}, \dots, s_{|S|+b}) \leftarrow \text{indices of the top-}b \text{ entries in } \mathbf{d}^{(t-1)}.$$

With  $\tau_b = 0$ , BGP is reduced to CPQR. For adversarial inputs like the one in Example 4.1, BGP tends to suffer from far worse skeleton complexities than those of BRP (Figure 1 (left)).

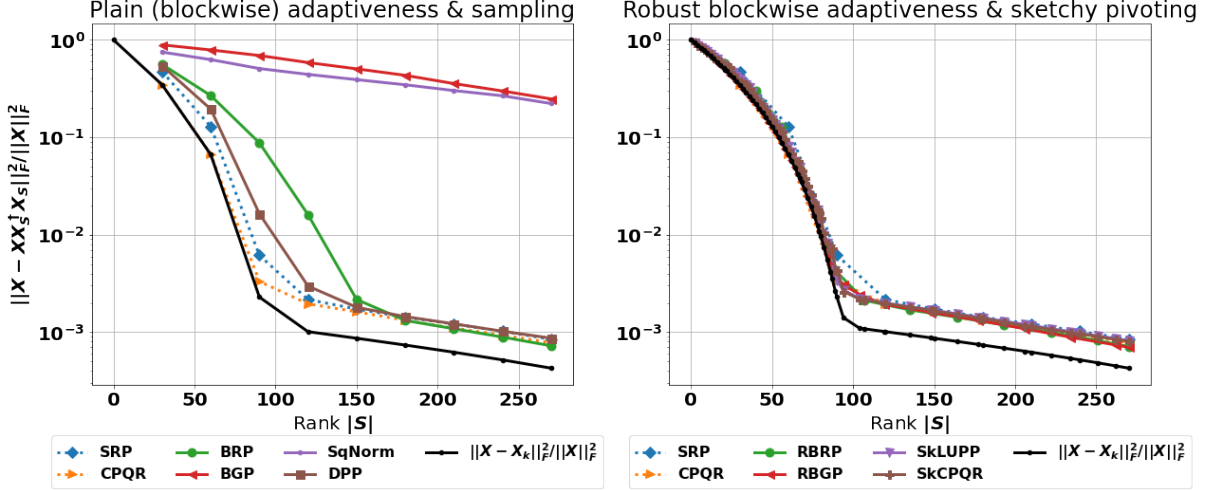


Figure 1: The skeletonization error  $\mathcal{E}_X(S)$  of algorithms in Table 2 on a GMM-based adversarial input as described in Example 4.1, where the adaptiveness is critical for achieving a good skeleton complexity/accuracy. **(Left)**: Sequential random pivoting (SRP) and greedy pivoting (CPQR) enjoy the best skeleton complexities. The plain blockwise random pivoting (BRP) and greedy pivoting (BGP) tend to suffer from observably higher skeleton complexities than the sequential adaptive methods, while greedy selection tends to severely exacerbate such inefficiency. The squared-norm sampling (SqNorm) can be viewed as plain BRP with block size  $b = k$ , which suffers from a similar inefficiency as BRP/BGP. DPP sampling attains relatively good accuracy even without adaptiveness, thanks to its nearly optimal skeleton complexity [2, 5, 21], but with a much higher runtime in practice as a trade-off (e.g., with [17], k-DPP takes about  $10^3 \times$  longer than other algorithms in Table 2). **(Right)**: With robust blockwise filtering (Remark 4.1), robust blockwise random pivoting (RBRP) and greedy pivoting (RBGP), as well as the sketchy pivoting algorithms, achieves the comparable, nearly optimal skeleton complexities as the sequential adaptive methods. It is worth highlighting that despite the comparable skeleton complexities between RBRP and RBGP, RBGP is generally much slower than RBRP (cf. Figure 2). This is because, without randomness, blockwise greedy pivoting tends to pick more redundant points in each block, which are later filtered out.

By comparing Figure 1 (left) and (right), we observe that the robust blockwise filtering (Remark 4.1) brings improvement for both blockwise random and greedy pivoting. In particular, with  $\tau_b = \frac{1}{b}$ , RBRP (and RBGP) empirically attains comparable skeleton complexities as those of the sequential random pivoting on the GMM adversarial input (Example 4.1). The same observation extends to all the natural and synthetic data matrices tested in our experiments (Section 6), which leads to the following Conjecture 4.1:

**Conjecture 4.1** (Skeleton complexity of RBRP). *RBRP (Algorithm 4.1) with  $\tau_b = \frac{1}{b}$  shares a similar skeleton complexity as sequential random pivoting (Proposition 3.1) in expectation.*

*Rationale for Conjecture 4.1.* Consider Algorithm 4.1 at the  $t$ -th step with  $|S|$  selected skeletons from the previous steps,  $|S_t| = b$  candidates drawn from  $\frac{\mathbf{d}^{(t-1)}}{\|\mathbf{d}^{(t-1)}\|_1}$ , and  $|S'_t| = b'$  remaining skeletons in  $S_t$  that pass through the robust blockwise filtering (Remark 4.1). Now suppose we switch to sequential random pivoting after the  $(t-1)$ -th step and draw  $b'$  skeletons



adaptively, denoted as  $S_t''$ . Then, the key rationale for Conjecture 4.1 is that with  $\tau_b = \frac{1}{b}$ ,  $\mathcal{E}_{\mathbf{X}}(S \cup S_t') \approx \mathcal{E}_{\mathbf{X}}(S \cup S_t'')$  with (a reasonably) high probability.

To see this, we observe the close connection between the selection scheme of  $S_t'$  and that of  $S_t''$ :

- The robust blockwise filtering for  $S_t'$  in RBRP adaptively selects the point with the maximum residual norm in each step (*i.e.*, CPQR on the residual matrix  $\mathbf{V}$  in Algorithm 4.1), within a small subset  $S_t$  of  $b$  points sampled according to the squared-norm distribution over  $[n] \setminus S$ .
- The random pivoting for  $S_t''$  in SRP adaptively selects the point according to the squared-norm distribution of the residual over the complement of the skeleton subset in each step.

Intuitively, every selection made for  $S_t'$  and  $S_t''$  brings similar decay in the skeletonization error if the squared norms of the residual matrix corresponding to remaining points in  $S_t$  are around the maxima in the complement of the skeleton subset such that these remaining points in  $S_t$  can be selected by SRP with high probability<sup>8</sup>. Instead of computing the squared norms of the entire residual matrix explicitly for each selection as SRP (which leads to the undesired sequential updates), RBRP leverages the threshold  $\tau_b = \frac{1}{b}$  to encourage that the first  $b'$  points selected by the robust blockwise filtering in each block have such top squared norms in the corresponding residual matrices. Notice that with  $\tau_b = \frac{1}{b}$ , we enforce the sum of squared norms of the  $b'$  points to be larger than the average squared norm of the original block:  $\|\mathbf{R}_{\mathbf{V}}(i : b, i : b)\|_F^2 \geq \frac{1}{b} \|\mathbf{V}\|_F^2$ . Since the squared norms of residuals are non-increasing under QR updates,  $\frac{1}{b} \|\mathbf{V}\|_F^2$  serves as an overestimate for the squared norms of redundant points sampled in  $S_t$ .

As toy examples, if  $\mathbf{V}$  is rank deficient (*i.e.*,  $\text{rank}(\mathbf{V}) = b' < b$ ), then there exists  $b' \leq b''$  such that  $\|\mathbf{R}_{\mathbf{V}}(b' : b, b' : b)\|_F^2 \geq \frac{1}{b} \|\mathbf{V}\|_F^2$  but

$$0 = \|\mathbf{R}_{\mathbf{V}}(b'' + 1 : b, b'' + 1 : b)\|_F^2 \leq \|\mathbf{R}_{\mathbf{V}}(b' + 1 : b, b' + 1 : b)\|_F^2 < \frac{1}{b} \|\mathbf{V}\|_F^2.$$

Meanwhile, if  $\mathbf{V} \in \mathbb{R}^{d \times b}$  contains orthogonal columns with the same squared norm, then  $\|\mathbf{R}_{\mathbf{V}}(i : b, i : b)\|_F^2 \geq |\mathbf{R}_{\mathbf{V}}(b, b)|^2 = \frac{1}{b} \|\mathbf{V}\|_F^2$  for all  $i \in [b]$ , and therefore  $b' = b$ . ■

## 5 Interpolation Matrix Construction

In this section, we consider the construction of the interpolation matrix  $\mathbf{W}$  after skeleton selection. In particular, we are interested in exploiting information from the  $O(ndk)$  skeleton selection algorithms in Table 1, *i.e.*, the matrix  $\mathbf{L} \in \mathbb{R}^{n \times k}$  in Algorithms 3.1, 3.3 and 4.1, to construct  $\mathbf{W}$  efficiently in  $O(nk^2)$  time.

We begin by noticing the optimal interpolation matrix follows the least square problem

$$\min_{\mathbf{W} \in \mathbb{R}^{n \times k}} \|\mathbf{X} - \mathbf{W}\mathbf{X}_S\|_F^2 \quad \Rightarrow \quad \mathbf{W} = \mathbf{X}\mathbf{X}_S^\dagger = \mathbf{X}\mathbf{X}_S^\top (\mathbf{X}_S\mathbf{X}_S^\top)^{-1}, \quad (9)$$

so that we can compute such optimal  $\mathbf{W}$  exactly in  $O(ndk + dk^2 + nk^2)$  time via QR decomposition on  $\mathbf{X}_S$ . However, the dominant cost  $O(ndk)$  requires additional passes through  $\mathbf{X}$  and can be prohibitive after the skeleton selection stage.

<sup>8</sup>It is worth mentioning that, in contrast to SRP, RBRP does not recompute the entire residual matrix after each skeleton selection. Instead, within each block, RBRP computes the residual matrix locally for  $\mathbf{X}(S_t, :)$  only, while updating the entire residual matrix at the end of each block via matrix-matrix multiplication.

## 5.1 Exact-ID-revealing Algorithms

With the output matrix  $\mathbf{L} \in \mathbb{R}^{n \times k}$  from Algorithms 3.1 and 4.1, the corresponding optimal interpolation matrix  $\mathbf{X}\mathbf{X}_S^\dagger$  can be computed in  $O(nk^2)$  time following Algorithm 5.1.

---

### Algorithm 5.1 Interpolation matrix construction (ID)

---

**Require:** (a)  $\boldsymbol{\pi} \in \mathfrak{S}_n$  (such that  $S = \boldsymbol{\pi}(1:k)$ ), (b)  $\mathbf{L} \in \mathbb{R}^{n \times k}$ ,

**Ensure:** (a)  $\mathbf{W} \in \mathbb{R}^{n \times k}$

1:  $\mathbf{L}_1 \leftarrow \mathbf{L}(\boldsymbol{\pi}(1:k), :) \in \mathbb{R}^{k \times k}$ ,  $\mathbf{L}_2 \leftarrow \mathbf{L}(\boldsymbol{\pi}(k+1:n), :) \in \mathbb{R}^{(n-k) \times k}$

2:  $\mathbf{W} \leftarrow \mathbf{0}_{n \times k}$ ,  $\mathbf{W}(\boldsymbol{\pi}(1:k), :) = \mathbf{I}_k$

3:  $\mathbf{W}(\boldsymbol{\pi}(k+1:n), :) = \mathbf{L}_2\mathbf{L}_1^{-1}$   $\triangleright O(nk^2)$

---

**Proposition 5.1.** *The sequential (Algorithm 3.1) and blockwise (Algorithm 4.1) random pivoting, as well as their greedy pivoting variations, are exact-ID-revealing (Definition 1.2).*

*Proof of Proposition 5.1.* We first observe that the difference between sequential/blockwise random versus greedy pivoting lies only in the skeleton subset  $S$ . That is, assuming the same skeleton selection  $S$ , the resulting  $\mathbf{L}$ 's from random and greedy pivoting would be the same. Therefore, it is sufficient to show that Proposition 5.1 holds for random pivoting in Algorithms 3.1 and 4.1.

For both Algorithms 3.1 and 4.1, recall that  $\mathbf{L} \leftarrow \mathbf{L}^{(t)}$ . We observe that  $\mathbf{L}\mathbf{Q}^{(t)\top}$  provides a rank- $k$  approximation for  $\mathbf{X}$ :  $\|\mathbf{X} - \mathbf{L}\mathbf{Q}^{(t)\top}\|_F^2 = \|\mathbf{d}^{(t)}\|_1 = \mathcal{E}_{\mathbf{X}}(S) < \tau \|\mathbf{X}\|_F^2$ . We will show that  $\mathbf{L}\mathbf{Q}^{(t)\top} = \mathbf{X}\mathbf{X}_S^\dagger$  in exact arithmetic.

Then, with  $\mathbf{L}_1 \leftarrow \mathbf{L}(\boldsymbol{\pi}(1:k), :)$  and  $\mathbf{L}_2 \leftarrow \mathbf{L}(\boldsymbol{\pi}(k+1:n), :)$  as in Algorithm 5.1, by constructing,  $\mathbf{L}_2\mathbf{Q}^{(t)\top} = \mathbf{X}(\boldsymbol{\pi}(k+1:n), :)$  and  $\mathbf{L}_1\mathbf{Q}^{(t)\top} = \mathbf{X}_S = \mathbf{X}(\boldsymbol{\pi}(1:k), :)$  where  $\mathbf{L}_1 \in \mathbb{R}^{k \times k}$  is invertible as  $\mathbf{X}_S$  consists of linearly independent rows. Therefore,  $\mathbf{X}_S^\dagger = \mathbf{Q}^{(t)}\mathbf{L}_1^{-1}$ , and the optimal interpolation matrix  $\mathbf{W} = \mathbf{X}\mathbf{X}_S^\dagger$  can be expressed up to permutation as

$$\mathbf{W}(\boldsymbol{\pi}, :) = \mathbf{X}(\boldsymbol{\pi}, :)\mathbf{X}_S^\dagger = \begin{bmatrix} \mathbf{L}_1\mathbf{Q}^{(t)\top} \\ \mathbf{L}_2\mathbf{Q}^{(t)\top} \end{bmatrix} \mathbf{Q}^{(t)}\mathbf{L}_1^{-1} = \begin{bmatrix} \mathbf{L}_1 \\ \mathbf{L}_2 \end{bmatrix} \mathbf{L}_1^{-1} = \begin{bmatrix} \mathbf{I}_k \\ \mathbf{L}_2\mathbf{L}_1^{-1} \end{bmatrix}.$$

The computation of  $\mathbf{L}_2\mathbf{L}_1^{-1}$  involves solving a small  $k \times k$  system  $(n-k)$  times, which takes  $O(nk^2)$  time in general. Overall, given  $\mathbf{L}$  from Algorithms 3.1 and 4.1, Algorithm 5.1 constructs the optimal interpolation matrix  $\mathbf{W} = \mathbf{X}\mathbf{X}_S^\dagger = \mathbf{L}\mathbf{L}_1^{-1}$ . ■

Moreover, the special structure of  $\mathbf{L}_1$  may be leveraged to further accelerate the construction of  $\mathbf{W}$ . For instance,  $\mathbf{L}_1$  from the sequential algorithm in Algorithm 3.1 is lower triangular, where  $\mathbf{L}_2\mathbf{L}_1^{-1}$  can be evaluated via backward substitution in  $O((n-k)k^2)$  time.

However, for the blockwise algorithm in Algorithm 4.1 with a reasonably large block size  $b$ ,  $\mathbf{L}_1$  tends to be ill-conditioned in practice due to numerical error, where truncated SVD is usually necessary for numerical stability, as elaborated in Remark 5.1.

**Remark 5.1** (Evaluation of  $\mathbf{L}_2\mathbf{L}_1^{-1}$  for (R)BRP). *In Algorithm 4.1,  $\widehat{\mathbf{L}}^{(t)}(\boldsymbol{\pi}_a, :) \leftarrow \mathbf{X}(\boldsymbol{\pi}_a, :)\mathbf{Q}_V$  leads to a  $b$ -block lower triangular (instead of lower triangular)  $\mathbf{L}_1$ , where  $\mathbf{L}_2\mathbf{L}_1^{-1}$  can be computed via QR or (truncated) SVD of  $\mathbf{L}_1$  in  $O(nk^2)$  time. Specifically, when  $\mathbf{L}_1$  is ill-conditioned,*

we evaluate  $\mathbf{L}_1^{-1}$  via truncated SVD with small singular value clipping for numerical stability, which takes  $O(nk^2 + k^3)$  time<sup>9</sup>.

Alternatively, one can manually triangularize  $\mathbf{L}_1$  via an additional QR when computing  $\widehat{\mathbf{L}}^{(t)}(\boldsymbol{\pi}_a, :)$  in each block:

$$\sim, \widehat{\mathbf{L}}^{(t)}(\boldsymbol{\pi}_a, :)^{\top} \leftarrow \text{qr} \left( (\mathbf{X}(\boldsymbol{\pi}_a, :)\mathbf{Q}_V)^{\top}, \text{“econ”} \right), \quad (10)$$

with an additional cost of  $O(nkb)$  in total. When such lower triangularized  $\mathbf{L}_1$  is well-conditioned,  $\mathbf{L}_2\mathbf{L}_1^{-1}$  can be evaluated efficiently and stably via backward substitution. However, with a reasonably large block size  $b$  for the sake of parallelizability in practice, the resulting triangular matrix  $\mathbf{L}_1$  tends to be ill-conditioned or even numerically singular due to numerical error, where truncated SVD is nevertheless necessary for the stable construction of  $\mathbf{L}_2\mathbf{L}_1^{-1}$ .

## 5.2 Inexact-ID-revealing Algorithms

In contrast to Algorithms 3.1 and 4.1,  $\mathbf{L}$  from the sketchy pivoting algorithms in Algorithm 3.3 is insufficient for computing the optimal interpolation matrix  $\mathbf{X}\mathbf{X}_S^{\dagger}$  exactly, intuitively due to the loss of information in sketching (*i.e.*, randomized dimension reduction).

**Proposition 5.2.** *The sketchy pivoting algorithms (Algorithm 3.3) are inexact-ID-revealing.*

Proposition 5.2 follows directly from the observation that applying Algorithm 5.1 on  $\mathbf{L}$  from Algorithm 3.3 (*i.e.*,  $\mathbf{W} = \mathbf{L}\mathbf{L}_1^{-1}$ ) solves a sketched version of Equation (9):

$$\min_{\mathbf{W} \in \mathbb{R}^{n \times k}} \left\| \mathbf{X}\widehat{\boldsymbol{\Omega}} - \mathbf{W}\mathbf{X}_S\widehat{\boldsymbol{\Omega}} \right\|_F^2 \Rightarrow \mathbf{W} = \mathbf{L}\mathbf{L}_1^{-1} = \mathbf{X}\widehat{\boldsymbol{\Omega}} \left( \mathbf{X}_S\widehat{\boldsymbol{\Omega}} \right)^{\dagger}, \quad (11)$$

where  $\widehat{\boldsymbol{\Omega}} = \boldsymbol{\Omega}(:, 1:k) \in \mathbb{R}^{d \times k}$  consists of the first  $k$  columns in the randomized linear embedding  $\boldsymbol{\Omega} \in \mathbb{R}^{d \times l}$  drawn in Algorithm 3.3. Unfortunately, such sketched least square estimation [14, 37, 46] is known to be suboptimal as long as  $l < d$  [35].

Specifically for the interpolation matrix construction, the sketched estimation with a sample size as small as  $k$  (*i.e.*, without oversampling) in Algorithm 3.3 leads to a large interpolation error  $\mathcal{E}_{\mathbf{X}}(\mathbf{W} | S) \gg \mathcal{E}_{\mathbf{X}}(S)$ , as numerically illustrated in Section 6.2 (*e.g.*, comparing  $\mathcal{E}_{\mathbf{X}}(\mathbf{W} | S)$  as SkCPQR/SkLUPP-ID in Figure 2 and  $\mathcal{E}_{\mathbf{X}}(S)$  as SkCPQR/SkLUPP in Figure 1 (right)).

As an intuitive but effective remedy, the oversampled sketchy ID (OSID) in Algorithm 5.2 generalizes Algorithm 5.1 by increasing the sample size beyond  $k$  (*i.e.*, oversampling), which is shown to considerably alleviate such suboptimality of Equation (11) in interpolation error  $\mathcal{E}_{\mathbf{X}}(\mathbf{W} | S)$  (*cf.* Section 6.2, SkCPQR/SkLUPP-ID versus -OSID in Figures 2 to 6). Concretely, with a moderate multiplicative oversampling  $l = O(k)$  (*e.g.*,  $l = 2k$  in Figures 2 to 6 is usually sufficient in practice), Algorithm 5.2 can be expressed as

$$\text{OSID :} \quad \begin{aligned} \mathbf{Y}_S &= \mathbf{Y}(S, :), & \mathbf{Y}_S^{\top} &= \mathbf{Q} \mathbf{R} \\ k \times l & & l \times k & \quad l \times k \quad k \times k \\ \mathbf{W} &= \mathbf{Y}\mathbf{Y}_S^{\dagger} = (\mathbf{Y}\mathbf{Q})\mathbf{R}^{-\top} = \mathbf{X}(\boldsymbol{\Omega}\boldsymbol{\Omega}^{\top})\mathbf{X}_S^{\dagger} \end{aligned} \quad (12)$$

<sup>9</sup>In the common low-rank approximation scenario with  $k \ll n$ , the lower order term  $k^3 \ll nk^2$ , and therefore constructing the interpolation matrix via truncated SVD maintains the  $O(nk^2)$  complexity asymptotically.

---

**Algorithm 5.2** Oversampled sketchy interpolation matrix construction (OSID)

---

**Require:** (a)  $\pi \in \mathfrak{S}_n$  ( $S = \pi(1:k)$ ), (b) Sample size  $l \geq k$  (or pre-computed  $\mathbf{Y} \in \mathbb{R}^{n \times l}$ )

**Ensure:** (a)  $\mathbf{W} \in \mathbb{R}^{n \times k}$

1: (Draw a randomized linear embedding  $\Omega \in \mathbb{R}^{d \times l}$ )

2: ( $\mathbf{Y} \leftarrow \mathbf{X}\Omega \in \mathbb{R}^{n \times l}$ )

3:  $\mathbf{Q}, \mathbf{R} \leftarrow \text{qr} \left( \mathbf{Y}(\pi(1:k), :)^{\top}, \text{“econ”} \right) \quad \triangleright \mathbf{Q} \in \mathbb{R}^{l \times k}, \mathbf{R} \in \mathbb{R}^{k \times k}, O(lk^2)$

4:  $\mathbf{W} \leftarrow \mathbf{0}_{n \times k}, \mathbf{W}(\pi(1:k), :) = \mathbf{I}_k$

5:  $\mathbf{W}(\pi(k+1:n), :) \leftarrow (\mathbf{Y}(\pi(k+1:n), :) \mathbf{Q}) \mathbf{R}^{-\top} \quad \triangleright O((n-k)(lk+k^2))$

---

where  $\mathbb{E}_{\Omega}[\mathbf{W}] = \mathbf{X}\mathbf{X}_S^{\dagger}$  is an unbiased estimate for the optimal interpolation matrix when the embedding  $\Omega$  is isotropic, *i.e.*,  $\mathbb{E}_{\Omega}[\Omega\Omega^{\top}] = \mathbf{I}_d$ .

Leveraging the existing theories for randomized linear embedding, [46, Theorem 9 and 23] implies that with Equation (12), the gap between the interpolation and skeletonization errors converges as  $\mathcal{E}_{\mathbf{X}}(\mathbf{W} | S) - \mathcal{E}_{\mathbf{X}}(S) = O(k^2/l)$  when  $\Omega$  is a sparse embedding and  $l \gg k^2$ , whereas such convergence can be further improved to  $\mathcal{E}_{\mathbf{X}}(\mathbf{W} | S) - \mathcal{E}_{\mathbf{X}}(S) = O(k/l)$  with Gaussian embeddings (*e.g.*, by [46, Theorem 6]).

Asymptotically, Algorithm 5.2 takes  $O(nlk + nk^2 + lk^2) = O(nk^2 + k^3)$  time. Compared to Algorithm 5.1 without oversampling, the dominant cost  $O(nk^2)$  increases proportionally to the oversampling factor  $l/k$ . Nevertheless, such additional cost is affordable in practice (*cf.* Figures 2 to 6 (right)) thanks to the parallelizability of matrix-matrix multiplications [19].

## 6 Experiments

### 6.1 Data Matrices

In the experiments, we compare the accuracy and efficiency of various ID algorithms on several types of data matrices, including the matrix forms of natural image datasets and synthetic random matrices with varied spectra, outlined as follows.

1. We draw a synthetic random data matrix  $\mathbf{X} \in \mathbb{R}^{2000 \times 500}$  from the adversarial GMM described in Example 4.1 with  $k = 100$  cluster centers, denoted as GMM.
2. Recall that the MNIST training set [28] consists of 60,000 images of hand-written digits from 0 to 9. We denote MNIST as a data matrix consisting of  $n = 1000$  random images sampled uniformly from the MNIST training set where each row contains a flattened and *normalized*  $28 \times 28$  image such that  $d = 784$ . The nonzero entries take approximately 20% of the matrix.
3. The CIFAR-10 training set [26] consists of 60,000 colored images of size  $32 \times 32 \times 3$ . We denote CIFAR-10 as a data matrix consisting of  $n = 1000$  random images sampled uniformly from the CIFAR-10 training set where each row contains a flattened and *normalized* image such that  $d = 3072$ .
4. Let Gaussian-exp be a random dense data matrix of size  $1000 \times 1000$  with exponential spectral decay. We construct Gaussian-exp from its SVD  $\mathbf{X} = \mathbf{U}\Sigma\mathbf{V}^{\top}$  where

$\mathbf{U}, \mathbf{V} \in \mathbb{R}^{1000 \times 1000}$  are random unitary matrices drawn from the Haar measure, and  $\Sigma = \text{diag}(\sigma_1, \dots, \sigma_{1000})$  where  $\sigma_i = 1$  for all  $i \leq 100$  and  $\sigma_i = 0.8^{i-100}$  for all  $i > 100$ .

5. Let  $\text{SNN}$  be a random sparse non-negative (SNN) matrix [40] of size  $1000 \times 1000$  such that

$$\mathbf{X} = \sum_{i=1}^{100} \frac{10}{i} \mathbf{u}_i \mathbf{v}_i^T + \sum_{i=101}^{1000} \frac{1}{i} \mathbf{u}_i \mathbf{v}_i^T \quad (13)$$

where  $\mathbf{U} = [\mathbf{u}_1, \dots, \mathbf{u}_{1000}]$  and  $\mathbf{V} = [\mathbf{v}_1, \dots, \mathbf{v}_{1000}]$  are  $1000 \times 1000$  random sparse matrices with non-negative entries and sparsity 0.1.

## 6.2 Accuracy and Efficiency of ID

In Figures 2 to 6, we compare the empirical accuracy (left) and efficiency (right) of different ID algorithms on data matrices described in Section 6.1, with a focus on those demonstrating robust skeleton complexities on the adversarial input Example 4.1 (*i.e.*, algorithms in Figure 1 (right)).

Taking an integrated view of ID including skeleton selection and interpolation matrix construction, we consider the following relative ID error<sup>10</sup> and runtime measurements:

- (a) For error-revealing algorithms (*i.e.*, except for sketchy pivoting and sampling)<sup>11</sup>, we plot the residual errors (denoted as **residual**) from their on-the-fly skeletonization error estimates and the runtimes for skeleton selection (*e.g.*,  $\|\mathbf{d}^{(t)}\|_1$  in Algorithm 4.1) only.
- (b) For exact-ID-revealing algorithms (*i.e.*, except for sketchy pivoting and sampling), we plot the runtimes and interpolation errors  $\mathcal{E}_{\mathbf{X}}(\mathbf{W} | S)$  with  $\mathbf{W}$  from Algorithm 5.1 (**ID**), which are equal to the corresponding skeletonization errors  $\mathcal{E}_{\mathbf{X}}(\mathbf{W} | S) = \mathcal{E}_{\mathbf{X}}(S)$ .
- (c) For inexact-ID-revealing algorithms (*i.e.*, sketchy pivoting), we plot the runtimes and interpolation errors  $\mathcal{E}_{\mathbf{X}}(\mathbf{W} | S)$  with  $\mathbf{W}$  from both Algorithm 5.1 (**ID**) and Algorithm 5.2 (**OSID**) with small multiplicative oversampling  $l = 2k$ , where both  $\mathcal{E}_{\mathbf{X}}(\mathbf{W} | S) > \mathcal{E}_{\mathbf{X}}(S)$ , and Algorithm 5.2 tends to be more expensive.
- (d) For non-ID-revealing algorithms (*i.e.*, sampling), without explicitly specifying in the legends, we plot the runtimes and interpolation errors  $\mathcal{E}_{\mathbf{X}}(\mathbf{W} | S) = \mathcal{E}_{\mathbf{X}}(S)$  with the optimal  $\mathbf{W}$  from solving the exact least square problem in Equation (9).

The legends in Figures 2 to 6 are formatted in terms of “skeleton selection algorithm”-“ID error”. The abbreviations of different skeleton selection algorithms are summarized in Table 2, whereas the ID error measurements are described as above.

**Remark 6.1** (Choice of block size). *The choice of block size  $b$  controls the trade-off between parallelizability and error-revealing property. Precisely, an insuitably small  $b$  tends to fail exploiting the efficiency of matrix-matrix multiplications, whereas the larger  $b$  leads to higher overestimation on the target rank. In the experiments, we use  $b = 30$  or  $40$  to exploit the parallelizability of matrix-matrix multiplications without considerably compromising the error-revealing property.*

<sup>10</sup>All error measurements are normalized with  $\|\mathbf{X}\|_F^2$  to relative errors.

<sup>11</sup>In Figures 2 to 6, we also omit the residual errors of the sequential error-revealing algorithms SRP and CPQR (which overlap with the corresponding interpolation errors) for conciseness of demonstration.

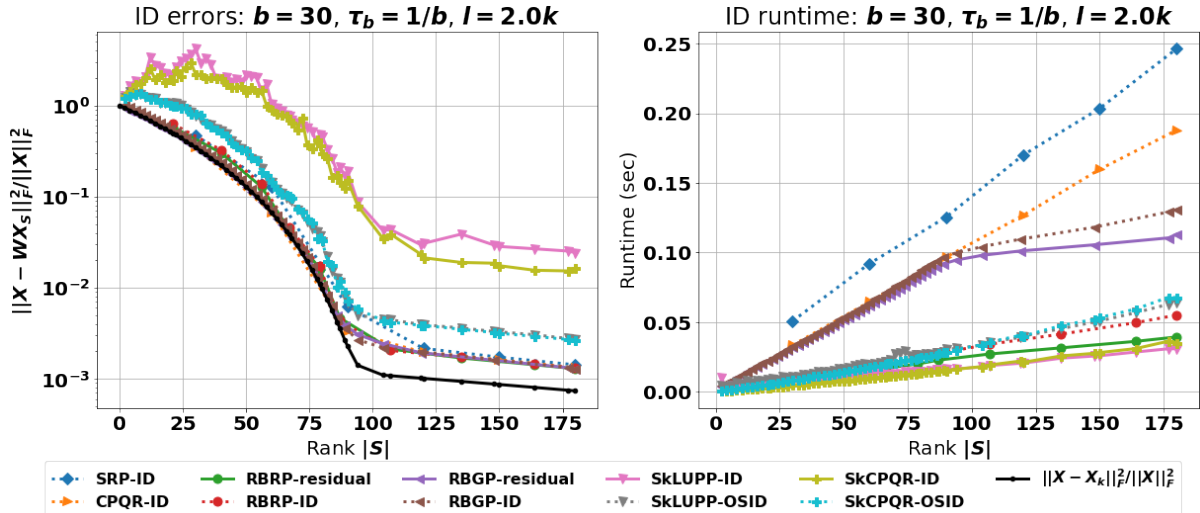


Figure 2: Relative interpolation error and runtime of ID algorithms with robust skeleton complexities on the GMM adversarial input (Example 4.1). Recall from Figure 1 that sampling methods, especially squared-norm sampling, suffer from significantly higher skeleton complexities than sequential/robust blockwise random pivoting and sketchy pivoting on GMM. For demonstration, we omit squared-norm sampling from the plot.

For the GMM adversarial input in Figure 2, it is worth pointing out that the sharp transition of RBGP at  $|S| \approx 100$  is because GMM consists of 100 clusters, each with distinct squared-norms. Recall that blockwise greedy pivoting picks points with the maximum norms without randomness. When  $|S| \leq 100$ , each block drains points from the same clusters with the maximum residual norms first, most of which are redundant points and are later excluded by the robust blockwise filtering. This leads to the inefficiency of RBGP when  $|S| \leq 100$ . While after  $|S| > 100$ ,  $S$  contains at least one skeleton from each of the 100 clusters. Therefore, the residuals are approximately *i.i.d.* Gaussian noise where RBGP works similarly to RBRP. Such inefficiency of RBGP in comparison to RBRP again illustrates the superiority of random pivoting over greedy pivoting, *i.e.*, the merit of randomness.

From experiments on the (non-adversarial) natural and synthetic datasets in Figures 3 to 6, we observe the following (by algorithms):

- The **robust blockwise random pivoting (RBRP)** enjoys (one of) the best skeleton complexities, with the skeletonization error estimates aligning perfectly with the interpolation errors (left), demonstrating the error-revealing and exact-ID-revealing abilities of RBRP. The skeleton selection process of RBRP tends to take slightly longer than that of sketchy pivoting (SkLUPP/SkCPQR) with ID (which is not error-revealing and suffers from much larger interpolation errors than RBRP). However, RBRP is generally faster than sketchy pivoting (SkLUPP/SkCPQR) with small multiplicative oversampling (OSID), while enjoying lower interpolation error. Overall, RBRP is shown to provide the best combination of accuracy and efficiency when the explicit construction of ID (in contrast to the skeleton subset only) is inquired.
- The sketchy pivoting algorithms (**SkLUPP/SkCPQR**) also enjoy (one of) the best skeleton complexities, despite the lack of error-revealing ability and being inexact-ID-revealing (*i.e.*,

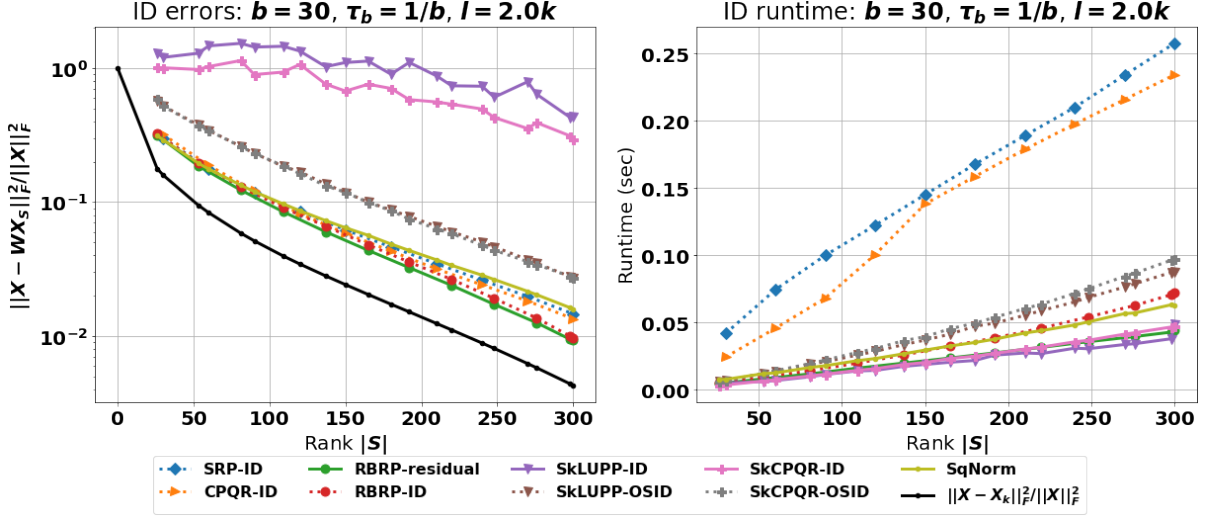


Figure 3: Relative interpolation error and runtime of ID algorithms on MNIST.

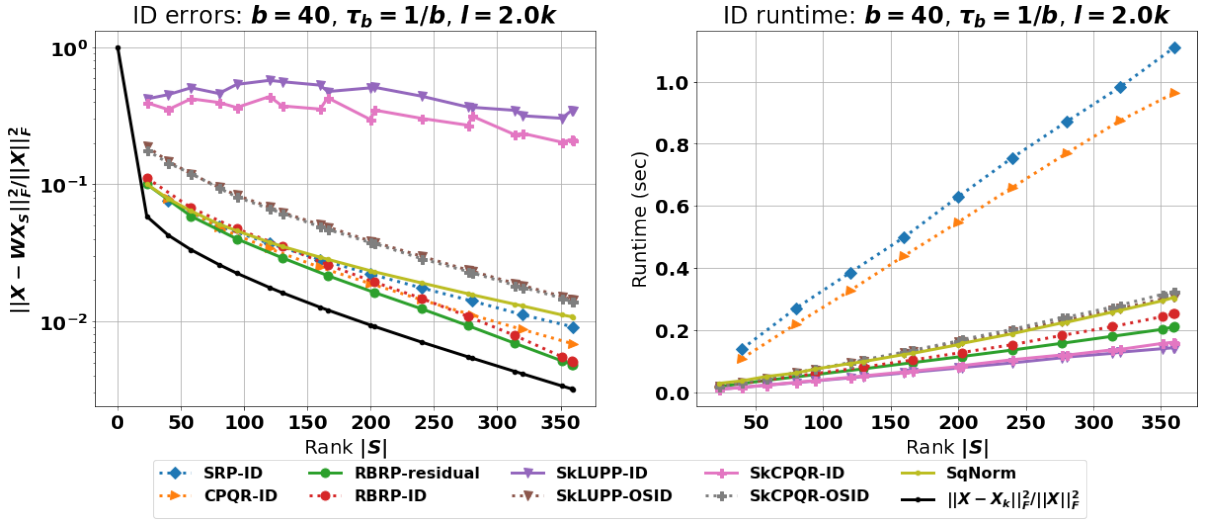


Figure 4: Relative interpolation error and runtime of ID algorithms on CIFAR-10.

suffering from large interpolation errors). That is, for skeleton selection only (without asking for the interpolation matrix), sketchy pivoting provides the most efficient selection of close-to-the-best skeleton subsets in practice (*cf.* Figure 1). Moreover, our experiments verify the conclusion in [15] that SkLUPP tends to be more efficient than SkCPQR in selecting skeletons without compromising the skeletonization error.

- The inherently sequential algorithms, including **SRP** and **CPQR**, are highly competitive in terms of accuracy while being considerably slower than the parallelizable ones.
- With appropriately normalized data, the  $O(nd)$ -time squared-norm sampling (**SqNorm**)<sup>12</sup>

<sup>12</sup>Although we follow Proposition 2.1 and show results by sampling  $k$  *i.i.d.* skeletons with *replacement*, in practice, we observe that sampling *without replacement* tends to provide better skeleton complexity, especially on the adversarial input Example 4.1. Intuitively, sampling without replacement can be viewed as a weaker version of adaptiveness where only the selected point itself is excluded from the future selection.

also provides highly competitive skeleton complexities, while constructing the interpolation matrix by solving Equation (9) explicitly can slow down the overall ID algorithm significantly to the extent that the runtimes are similar to those of RBRP. However, we recall that sampling methods are in lack of error-revealing and ID-revealing abilities. Moreover, SqNorm is vulnerable to adversarial inputs like Example 4.1, as shown in Figure 1.

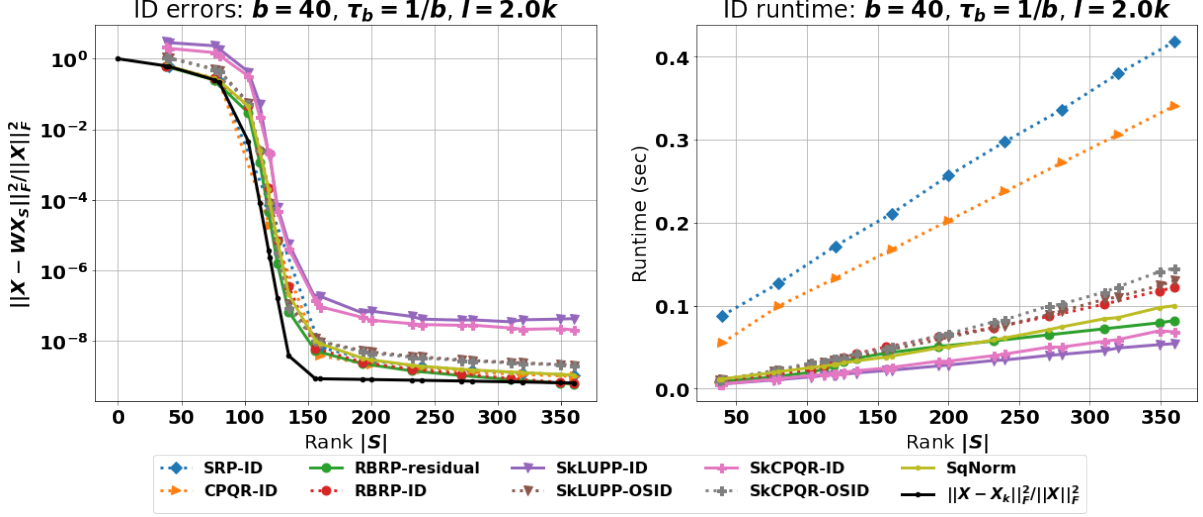


Figure 5: Relative interpolation error and runtime of ID algorithms on Gaussian-exp.

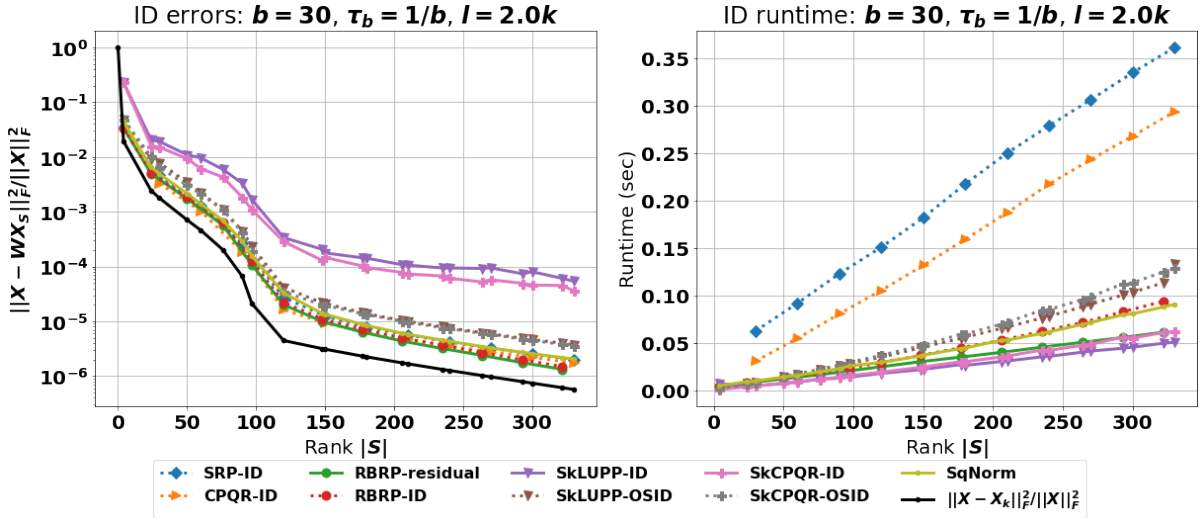


Figure 6: Relative interpolation error and runtime of ID algorithms on SNN.

## 7 Discussions and Future Directions

In this work, we focus on fast and accurate ID algorithms from five perspectives that measure the empirical performance systematically: (a) skeleton complexity, (b) asymptotic complexity, (c) parallelizability, (d) error-revealing property, and (e) ID-revealing property. With a careful exploration of various existing ID algorithms through the lens of adaptiveness and/or randomness, we reemphasize the effectiveness of combining adaptiveness and randomness in solving



ID problems, while unveiling a critical missing piece in the family of existing algorithms that masters all five aforementioned perspectives. To close the gap, we propose *robust blockwise random pivoting (RBRP)*—a parallelizable, error-revealing, and exact-ID-revealing algorithm that enjoys among-the-best skeleton and asymptotic complexities in practice compared to the existing algorithms and demonstrates promising robustness to adversarial inputs. With numerical experiments, we illustrate the empirical accuracy, efficiency, and robustness of RBRP on a broad spectrum of natural and synthetic datasets.

As an appealing future direction, rigorous proofs of Conjecture 3.2 and 4.1 could bring insights beyond formalizing the empirical successes of Algorithms 3.3 and 4.1. Specifically concerning Conjecture 3.2, greedy algorithms like pivoted LU and QR commonly suffer from scarce adversarial inputs (*e.g.*, Kahan-type matrices [25]) that severely compromise the worst-case performance. For ID, despite the competitive empirical skeleton complexity of greedy pivoting (CPQR), the worst-case skeleton complexity guarantee of CPQR scales proportionally to the problem size  $n$ , in contrast to the rank  $r \ll n$  for other methods involving randomness (*cf.* Table 1). Probabilistically circumventing the adversarial inputs via random perturbation, randomness (*e.g.*, random matrices [42] and additive Gaussian noise in smoothed analysis [39, 41]) is widely leveraged to quantify the scarceness of these adversarial inputs and explain the effectiveness of greedy methods in practice. Analogously for randomization via sketching, the proof of Conjecture 3.2 would provide theoretical justification for the robustness of greedy pivoting coupled with sketching by establishing an equivalence with random pivoting.

## Acknowledgments

YD was supported in part by the Office of Naval Research N00014-18-1-2354, NSF DMS-1952735, DOE ASCR DE-SC0022251, UT Austin Graduate School Summer Fellowship, and NYU Courant Instructorship. CC was supported in part by startup funds of North Carolina State University. KP was supported in part by the Peter O’Donnell Jr. Postdoctoral Fellowship at the Oden Institute. The authors wish to thank Ethan Epperly, Kevin Miller, Christopher Musco, Rachel Ward, and Robert Webber for enlightening discussions.

## References

- [1] D. Arthur and S. Vassilvitskii. K-means++ the advantages of careful seeding. In *Proceedings of the eighteenth annual ACM-SIAM symposium on Discrete algorithms*, pages 1027–1035, 2007.
- [2] M.-A. Belabbas and P. J. Wolfe. Spectral methods in machine learning and new strategies for very large datasets. *Proceedings of the National Academy of Sciences*, 106(2):369–374, 2009.
- [3] L. S. Blackford, A. Petitet, R. Pozo, K. Remington, R. C. Whaley, J. Demmel, J. Dongarra, I. Duff, S. Hammarling, G. Henry, et al. An updated set of basic linear algebra subprograms (blas). *ACM Transactions on Mathematical Software*, 28(2):135–151, 2002.
- [4] C. Boutsidis and A. Gittens. Improved matrix algorithms via the subsampled randomized

- hadamard transform. *SIAM Journal on Matrix Analysis and Applications*, 34(3):1301–1340, 2013.
- [5] Y. Chen, E. N. Epperly, J. A. Tropp, and R. J. Webber. Randomly pivoted cholesky: Practical approximation of a kernel matrix with few entry evaluations. *arXiv preprint arXiv:2207.06503*, 2022.
- [6] K. L. Clarkson and D. P. Woodruff. Low-rank approximation and regression in input sparsity time. *Journal of the ACM (JACM)*, 63(6):1–45, 2017.
- [7] M. B. Cohen, Y. T. Lee, C. Musco, C. Musco, R. Peng, and A. Sidford. Uniform sampling for matrix approximation. In *Proceedings of the 2015 Conference on Innovations in Theoretical Computer Science*, pages 181–190, 2015.
- [8] A. Cortinovis and D. Kressner. Low-rank approximation in the frobenius norm by column and row subset selection. *SIAM Journal on Matrix Analysis and Applications*, 41(4):1651–1673, 2020.
- [9] M. Dereziński. Fast determinantal point processes via distortion-free intermediate sampling. In *Conference on Learning Theory*, pages 1029–1049. PMLR, 2019.
- [10] M. Dereziński and M. W. Mahoney. Determinantal point processes in randomized numerical linear algebra. *Notices of the American Mathematical Society*, 68(1):34–45, 2021.
- [11] M. Dereziński, R. Khanna, and M. W. Mahoney. Improved guarantees and a multiple-descent curve for column subset selection and the nystrom method. *Advances in Neural Information Processing Systems*, 33:4953–4964, 2020.
- [12] A. Deshpande and S. Vempala. Adaptive sampling and fast low-rank matrix approximation. In *International Workshop on Approximation Algorithms for Combinatorial Optimization*, pages 292–303. Springer, 2006.
- [13] A. Deshpande, L. Rademacher, S. S. Vempala, and G. Wang. Matrix approximation and projective clustering via volume sampling. *Theory of Computing*, 2(1):225–247, 2006.
- [14] E. Dobriban and S. Liu. Asymptotics for sketching in least squares regression. *Advances in Neural Information Processing Systems*, 32, 2019.
- [15] Y. Dong and P.-G. Martinsson. Simpler is better: a comparative study of randomized algorithms for computing the cur decomposition. *arXiv preprint arXiv:2104.05877*, 2021.
- [16] P. Drineas, M. Magdon-Ismail, M. W. Mahoney, and D. P. Woodruff. Fast approximation of matrix coherence and statistical leverage. *The Journal of Machine Learning Research*, 13(1):3475–3506, 2012.
- [17] G. Gautier, G. Polito, R. Bardenet, and M. Valko. DPPy: DPP Sampling with Python. *Journal of Machine Learning Research - Machine Learning Open Source Software (JMLR-MLOSS)*, 2019. Code at <http://github.com/guilgautier/DPPy/> Documentation at <http://dppy.readthedocs.io/>.
- [18] G. H. Golub and C. F. Van Loan. *Matrix computations*. JHU press, 2013.

- [19] K. Goto and R. Van De Geijn. High-performance implementation of the level-3 blas. *ACM Transactions on Mathematical Software (TOMS)*, 35(1):1–14, 2008.
- [20] M. Gu and S. C. Eisenstat. Efficient algorithms for computing a strong rank-revealing qr factorization. *SIAM Journal on Scientific Computing*, 17(4):848–869, 1996.
- [21] V. Guruswami and A. K. Sinop. Optimal column-based low-rank matrix reconstruction. In *Proceedings of the twenty-third annual ACM-SIAM symposium on Discrete Algorithms*, pages 1207–1214. SIAM, 2012.
- [22] N. Halko, P.-G. Martinsson, and J. A. Tropp. Finding structure with randomness: Probabilistic algorithms for constructing approximate matrix decompositions. *SIAM review*, 53(2):217–288, 2011.
- [23] J. B. Hough, M. Krishnapur, Y. Peres, and B. Virág. Determinantal processes and independence. 2006.
- [24] P. Indyk and R. Motwani. Approximate nearest neighbors: towards removing the curse of dimensionality. In *Proceedings of the thirtieth annual ACM symposium on Theory of computing*, pages 604–613, 1998.
- [25] W. Kahan. Numerical linear algebra. *Canadian Mathematical Bulletin*, 9(5):757–801, 1966.
- [26] A. Krizhevsky, G. Hinton, et al. Learning multiple layers of features from tiny images. 2009.
- [27] A. Kulesza and B. Taskar. k-dpps: Fixed-size determinantal point processes. In *Proceedings of the 28th International Conference on Machine Learning (ICML-11)*, pages 1193–1200, 2011.
- [28] Y. LeCun. The mnist database of handwritten digits. <http://yann.lecun.com/exdb/mnist/>, 1998.
- [29] M. W. Mahoney and P. Drineas. Cur matrix decompositions for improved data analysis. *Proceedings of the National Academy of Sciences*, 106(3):697–702, 2009.
- [30] P.-G. Martinsson and J. A. Tropp. Randomized numerical linear algebra: Foundations and algorithms. *Acta Numerica*, 29:403–572, 2020.
- [31] P.-G. Martinsson, G. Quintana OrtI, N. Heavner, and R. Van De Geijn. Householder qr factorization with randomization for column pivoting (hqrrp). *SIAM Journal on Scientific Computing*, 39(2):C96–C115, 2017.
- [32] X. Meng and M. W. Mahoney. Low-distortion subspace embeddings in input-sparsity time and applications to robust linear regression. In *Proceedings of the forty-fifth annual ACM symposium on Theory of computing*, pages 91–100, 2013.
- [33] J. Nelson and H. L. Nguyễn. Osnap: Faster numerical linear algebra algorithms via sparser subspace embeddings. In *2013 IEEE 54th annual symposium on foundations of computer science*, pages 117–126. IEEE, 2013.

- [34] S. Oymak and J. A. Tropp. Universality laws for randomized dimension reduction, with applications. *Information and Inference: A Journal of the IMA*, 7(3):337–446, 2018.
- [35] M. Pilanci and M. J. Wainwright. Iterative hessian sketch: Fast and accurate solution approximation for constrained least-squares. *The Journal of Machine Learning Research*, 17(1):1842–1879, 2016.
- [36] G. Quintana-Ortí, X. Sun, and C. H. Bischof. A blas-3 version of the qr factorization with column pivoting. *SIAM Journal on Scientific Computing*, 19(5):1486–1494, 1998.
- [37] G. Raskutti and M. W. Mahoney. A statistical perspective on randomized sketching for ordinary least-squares. *The Journal of Machine Learning Research*, 17(1):7508–7538, 2016.
- [38] V. Rokhlin and M. Tygert. A fast randomized algorithm for overdetermined linear least-squares regression. *Proceedings of the National Academy of Sciences*, 105(36):13212–13217, 2008.
- [39] A. Sankar, D. A. Spielman, and S.-H. Teng. Smoothed analysis of the condition numbers and growth factors of matrices. *SIAM Journal on Matrix Analysis and Applications*, 28(2):446–476, 2006.
- [40] D. C. Sorensen and M. Embree. A deim induced cur factorization. *SIAM Journal on Scientific Computing*, 38(3):A1454–A1482, 2016.
- [41] D. A. Spielman and S.-H. Teng. Smoothed analysis: an attempt to explain the behavior of algorithms in practice. *Communications of the ACM*, 52(10):76–84, 2009.
- [42] L. N. Trefethen and R. S. Schreiber. Average-case stability of gaussian elimination. *SIAM Journal on Matrix Analysis and Applications*, 11(3):335–360, 1990.
- [43] J. A. Tropp. Improved analysis of the subsampled randomized hadamard transform. *Advances in Adaptive Data Analysis*, 3(01n02):115–126, 2011.
- [44] J. A. Tropp, A. Yurtsever, M. Udell, and V. Cevher. Fixed-rank approximation of a positive-semidefinite matrix from streaming data. *Advances in Neural Information Processing Systems*, 30, 2017.
- [45] S. Voronin and P.-G. Martinsson. Efficient algorithms for cur and interpolative matrix decompositions. *Advances in Computational Mathematics*, 43:495–516, 2017.
- [46] D. P. Woodruff et al. Sketching as a tool for numerical linear algebra. *Foundations and Trends® in Theoretical Computer Science*, 10(1–2):1–157, 2014.
- [47] F. Woolfe, E. Liberty, V. Rokhlin, and M. Tygert. A fast randomized algorithm for the approximation of matrices. *Applied and Computational Harmonic Analysis*, 25(3):335–366, 2008.